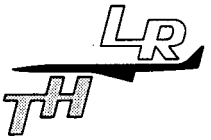

DELFT UNIVERSITY OF TECHNOLOGY

DEPARTMENT OF AEROSPACE ENGINEERING

Report LR-340

The stress distribution round an infinite row of circular holes in an orthotropic plate

by

Th. de Jong

DELFT - THE NETHERLANDS

january 1982

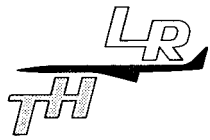

DELFT UNIVERSITY OF TECHNOLOGY

DEPARTMENT OF AEROSPACE ENGINEERING

Report LR-340

The stress distribution round an infinite row of circular holes in an orthotropic plate

by

Th. de Jong

DELFT - THE NETHERLANDS

january 1982

CONTENTS

SUMMARY

In this report an approximate solution is presented for the stresses round an infinite row of unloaded, equal circular holes in an orthotropic plate loaded at infinity. The calculations are based on the analytical method of complex stress functions.

The complex stress functions are evaluated from the boundary conditions of a single, central hole. The influence of the other holes is represented by Taylor-expansions of the elementary stress functions of these holes in the neighbourhood of the central hole. The use of series implies a limited accuracy of the solution. The numerical evaluation however shows that the convergence of the series is good.

The row of holes is oriented under an arbitrary angle with the symmetry axes of the material. Two loading conditions have been considered:

- a normal stress at infinity in a direction perpendicular to the row of holes,
- a normal strain at infinity in a direction perpendicular to the row of holes.

Numerical results are obtained for a number of carbon fibre reinforced laminates. The isotropic case has been added for reference purposes.

1. INTRODUCTION

The problem of generalized plane stress in an infinite orthotropic plate with a single hole has been solved by Lekhnitskii, Reference [1], by means of complex functions. As with isotropic materials the numerical results of infinite plate theory are often applied to plates containing a row of holes. For isotropic materials this is acceptable since the maximum stress concentration factor in the net area doesn't change significantly over a wide range of pitch to hole diameter ratio's. Furthermore in many isotropic materials yielding can take place in highly stressed regions, reducing the effect of stress concentrations on the net failing stress. In contrast modern composite materials tend to behave linearly almost up to failure or even exhibit a non-Hookean behaviour with increasing Young's modulus, Reference [2]. Therefore composite materials are very sensitive to stress risers which reduce the static strength considerably. Nevertheless the classical tensile stress concentration factor also has limited significance in predicting failure since other stress concentrations, e.g. the maximum shear stress concentration on the edge of the hole may cause failure. It is for instance well known that the tensile performance of a unidirectional strip with a circular hole is limited by the shear stress concentration in a point circa 10° from the net area and not by the extremely high tensile stress concentration of about 7 to 8 in the net area. On the other hand a ±45° laminate will fail due to the relatively low tensile stress concentration of about 2 in the net area. For strength predictions of composites based upon elastic analysis therefore accurate knowledge of the whole stress distribution around the hole is required.

In this paper the generalized plane stress problem of an infinite row of equal circular holes with equal spacing in an orthotropic plate is treated. The purpose is to investigate the interaction between the holes by varying the pitch to hole diameter ratio. The centre line of the holes coincides with the X-axis, the material symmetry axes in

general do not coincide with the coordinate axes. Two loading conditions have been chosen

- a normal stress σ_y at infinity,
- a normal strain ε_y at infinity resulting from p_y, $p_x = p_y \cdot C_{12} / C_{22}$ and $p_{xy} = p_y \cdot C_{26} / C_{22}$.

The approach to the problem has been adopted from Reference [3]. In the neighbourhood of the central hole the elementary complex stress functions of an arbitrary hole are expanded into Taylor series. Since an elementary function is a series with unknown coefficients, the expansion results in an infinite double sum with one set of unknown coefficients. For the whole periodic array of holes a complex stress function in the neighbourhood of the central hole is a triple sum. By satisfying the boundary conditions of the central hole, a system of linear equations is obtained. Solving a limited number of these equations results in an approximate solution of the stress functions.

In this report only four coefficients for both stress functions have been calculated. Nevertheless the accuracy of the solution seems to be technical acceptable. Calculations to verify this showed no differences in the numerical values of the stresses on the edge of the central hole in a three coefficient solution and the solution presented here. The values for the isotropic case fit well with values found in literature. It should be emphasized however that the Taylor expansions of the elementary stress functions of the single holes have limited areas of convergence around the central hole. For points outside this hole the four coefficients may not be sufficient, especially not for points near the edge of the convergence area. Therefore this solution is strictly limited to the edge of the central hole and its direct surrounding.

Numerical results have been obtained for five laminates of carbon fibre reinforced plastics, four pitch to hole diameter ratio's and two angles between material axes and coordinate axes. The mechanical

properties of the laminates are presented in Table 1, as well as two complex material parameters s_1 and s_2, needed in the theory of complex stress functions. The stresses for the two types of loading and the different geometrical conditions are presented graphically.

Although only two load conditions have been considered, it should be remarked that the present analysis is able to calculate stresses for any arbitrary combination of loads p_x, p_y and p_{xy} at infinity.

2. GENERAL EQUATIONS

The general theory on stress problems in orthotropic plates is discussed in detail in Reference [1]. A short summary of this theory is given here to make this paper selfcontained.

The boundary condition formulae for the loads on an orthotropic plate in a plane stress situation are

$$2\,\mathrm{Re}\sum_{k=1,2}\phi_k(z_k) = \int_0^s Y\,ds + K_1$$
$$2\,\mathrm{Re}\sum_{k=1,2} s_{k_\varphi}\,\phi_k(z_k) = -\int_0^s X\,ds + K_2 \qquad (2.1)$$

in which X and Y are external forces and $\phi_k(z_k)$ are complex functions of

$$z_k = x + s_{k_\varphi}\,y \qquad k = 1,2 \qquad (2.2)$$

After solving $\phi_k(z_k)$ the stresses can be calculated with

$$\sigma_x = 2\,\mathrm{Re}\sum_{k=1,2} s_{k_\varphi}^2\,\phi_k'(z_k)$$
$$\sigma_y = 2\,\mathrm{Re}\sum_{k=1,2} \phi_k'(z_k) \qquad (2.3)$$
$$\tau_{xy} = -2\,\mathrm{Re}\sum_{k=1,2} s_{k_\varphi}\,\phi_k'(z_k)$$

and the displacements in X- and Y-direction respectively with

$$U = 2\,\mathrm{Re} \sum_{k=1,2} U_{k_\varphi}\, \phi_k(z_k) + K_3 y + K_4$$
$$V = 2\,\mathrm{Re} \sum_{k=1,2} V_{k_\varphi}\, \phi_k(z_k) - K_3 x + K_5 \qquad (2.4)$$

The index φ denotes the angle φ between the material axes α-β and the coordinate axes. φ has a positive value when the material axes are rotated in clockwise direction relative to the coordinate axes.

K_1 ... K_5 are integration constants; K_3 is zero when no rotation of the plate as a rigid body is allowed. K_4 and K_5 represent a translation of the plate as a rigid body.

The complex constants s_{k_φ} are defined by

$$s_{k_\varphi} = \frac{s_k \cos\varphi - \sin\varphi}{s_k \sin\varphi + \cos\varphi} \qquad k = 1,2 \qquad (2.5)$$

in which s_k can be solved from

$$s_1^2 s_2^2 = \frac{s_{22}}{s_{11}}$$
$$s_1^2 + s_2^2 = -\frac{2s_{12} + s_{66}}{s_{11}} \qquad (2.6)$$

s_{ij} are the material compliances in the principal material directions. S_{k_φ} is either complex or imaginary.

In (2.4) is

$$U_k = s_{11_\varphi} s_{k_\varphi}^2 + s_{12_\varphi} - s_{16_\varphi} s_{k_\varphi} \qquad k = 1,2 \qquad (2.7)$$

$$V_k = s_{12_\varphi} s_{k_\varphi} + s_{22_\varphi} / s_{k_\varphi} - s_{26_\varphi}$$

in which s_{ij_φ} are the material compliances in the coordinate directions.

The general expressions for the elementary functions $\phi_k(z_k)$ in the case of an unloaded hole in an infinite orthotropic plate with non zero stresses at infinity are

$$\phi_k(z_k) = g_{-2}^{(k)} z_k^2 + g_{-1}^{(k)} z_k + g_0^{(k)} + \sum_{n=1,2}^{\infty} g_n^{(k)} z_k^{-n} \qquad (2.8)$$

The quadratic term in (2.8) is necessary if inplane bending moments are present. In the linear term, representing a homogeneous stress field is

$$g_{-1}^{(k)} = \frac{p_x - \frac{p_y}{2}\{(s_{\ell_\varphi}^2 + \bar{s}_{\ell_\varphi}^2) - (\bar{s}_{k_\varphi} + \bar{s}_{\ell_\varphi})(s_{\ell_\varphi} + \bar{s}_{\ell_\varphi})\} + p_{xy}(\bar{s}_{k_\varphi} + \bar{s}_{\ell_\varphi})}{(s_{k_\varphi} - s_{\ell_\varphi})(s_{k_\varphi} + s_{\ell_\varphi} - \bar{s}_{k_\varphi} - \bar{s}_{\ell_\varphi})} \qquad (2.9)$$

$k = 1,2$

$\ell = 3-k$

where p_x, p_y and p_{xy} are stresses at infinity.

The infinite series in (2.8) represents the influence of the hole. The unknown coefficients $g_n^{(k)}$ in these series must be solved from the boundary condition of the hole.

The constant $g_o^{(k)}$ in (2.8) has been added for formal reasons. For stress calculations it has no relevance.

3. THE COMPLEX STRESS FUNCTIONS FOR A ROW OF HOLES

The complex stress functions for a row of circular holes with equal spacing s can be considered as a sum of the elementary stress functions of the single holes. So, when the centre points of the holes are on the X-axis and the centre point of the central hole coincides with the origin of the coordinate system:

$$\phi_k^o(z_k) = \sum_{n=1,2}^{\infty} g_n^{(k)} z_k^{-n} + \sum_{m=1,2}^{\infty} \phi_k^m(z_k - ms) + \sum_{m=1,2}^{\infty} \phi_k^m(z_k + ms) \qquad (3.1)$$

$$k = 1,2$$

in which:

$\sum_{n=1,2}^{\infty} g_n^{(k)} z_k^{-n}$ are the elementary complex stress functions belonging to the central hole,

$\phi_k^m(z_k - ms)$ are the elementary complex stress functions belonging to the m-th hole to the right of the central hole,

$\phi_k^m(z_k + ms)$ are the elementary complex stress functions belonging to the m-th hole to the left of the central hole.

Since the row of holes is infinitely long and all holes are equal the elementary stress functions must be equal to the functions of the central hole, so:

$$\phi_k^m(z_k \pm ms) = \sum_{n=1,2}^{\infty} g_n^{(k)} (z_k \pm ms)^{-n} \qquad k = 1,2 \qquad (3.2)$$

N.B. The complex stress functions representing a single hole in an infinite plate with normal and shear loads at infinity along the

material axes have terms with odd, negative powers of z_k only. If the material axes and coordinate axes do not coincide the loads along the coordinate axes can always be transformed to the material axes. In that case the stress functions also have odd, negative powers of z_k. It is obvious that in a plate with a row of holes on the X-axis and an angle between material axes and coordinate axes the loads can also be transformed to the material axes. In that case however the geometry of the plate with holes is not symmetric with respect to the material axes. For that reason in the elementary stress functions of (3.1) and (3.2) terms with negative, even powers are included.

The coefficients $g_n^{(k)}$ in (3.1) and (3.2) must be obtained by satisfying the boundary conditions of one of the holes, for instance the central hole. The power series however produce very complicated expressions in z_k from which it is impossible to solve $g_n^{(k)}$. Therefore the stress functions of the holes to the left and to the right of the central hole are expanded in Taylor-series in an area around the centre of the coordinate system:

$$\phi_k^m(z_k \pm ms) = \sum_{p=0,1,2}^{\infty} \frac{z_k^p}{p!} \{\phi_k^{mp}(z_k \pm ms)\}_{z_k=0}$$

or, with (3.2)

$$\phi_k^m(z_k \pm ms) = \sum_{p=0,1,2}^{\infty} \frac{z_k^p}{p!} \sum_{n=1,2}^{\infty} (-n)(-n-1)\ldots(-n-p+1)\, g_n^{(k)} (\pm ms)^{-n-p} \qquad (3.3)$$

The terms with equal, odd powers of ms and -ms eliminate each other when (3.3) is substituted in (3.1). The terms with even values of -n-p are in pairs identical.

So, with $\sum_{p,n} = \sum_{p=0,2}^{\infty}\sum_{n=2,4}^{\infty} + \sum_{p=1,3}^{\infty}\sum_{n=1,3}^{\infty}$ (3.1) becomes:

$$\phi_k^o(z_k) = \sum_{n=1,2}^{\infty} g_n^{(k)} z_k^{-n} + \tag{3.4}$$

$$+ 2 \sum_{m=1,2}^{\infty} \sum_{p,n} \frac{z_k^p}{p!} (-n)(-n-1)\ldots(-n-p+1)\, g_n^{(k)} (-ms)^{-n-p}$$

On the edge of the hole $\frac{z_k^p}{p!}$ can be evaluated into the linear expression:

$$\frac{z_k^p}{p!} = \left(\frac{1-is_{k_\varphi}}{2}\right)^p \sum_{r=0,1} \frac{\lambda_k^r}{(p-r)!\,r!} \left\{\left(1+\lambda_k^{p-2r}\right) \cos(p-2r)\,\theta + \right. \tag{3.5}$$

$$\left. + i\left(1-\lambda_k^{p-2r}\right) \sin(p-2r)\,\theta\right\}$$

where

$$\lambda_k = \frac{1 + is_{k_\varphi}}{1 - is_{k_\varphi}} \tag{3.6}$$

and the upper limit of r is (p-1)/2 for p is odd and p/2-1 for p is even. The first series of (3.4) however still produces a complicated expression in sines and cosines on the edge of the central hole. Since this series contains only negative powers of z_k it may be replaced by a power series with only negative powers of

$$\zeta_k = \frac{z_k \pm \sqrt{z_k^2 - s_{k_\varphi}^2 - 1}}{1 - is_{k_\varphi}}$$

for which on the edge of the central hole

$$\zeta_1 = \zeta_2 = \sigma = \cos\theta + i \sin\theta$$

So

$$\sum_{n=1,2}^{\infty} g_n^{(k)} z_k^{-n} = \sum_{n=1,2}^{\infty} h_{n,o}^{(k)} \sigma^{-n} \qquad (3.8)$$

With

$$\sigma^{-n} = \cos n\theta - i \sin n\theta$$

(3.8) has now become rather simple on the edge of the central hole. However (3.8) introduces a new set of unknown coefficients $h_n^{(k)}$ in (3.4). Therefore the still present coefficients $g_n^{(k)}$ must be transformed in $h_n^{(k)}$ by the same transformation as used in (3.8):

$$\sum_n (-n)(-n-1).....(-n-p+1)\, g_n^{(k)} (-ms)^{-n-p}$$

$$= \frac{d^p}{d(-ms)^p} \sum_n g_n^{(k)} (-ms)^{-n} \qquad (3.9)$$

$$= \frac{d^p}{d(-ms)^p} \sum_n h_{n,o}^{(k)} \left\{ \frac{-ms - \sqrt{(ms)^2 - s_{k_\varphi}^2 - 1}}{1 - is_{k_\varphi}} \right\}^{-n}$$

where the - sign of (3.7) has been chosen because -ms has a negative value.

With (3.8) and (3.9) the stress functions for the row of holes are

$$\phi_k^o(z_k) = \sum_{n=1,2}^{\infty} h_{n,o}^{(k)}\, \sigma^{-n} + \tag{3.10}$$

$$+ 2 \sum_{m=1,2}^{\infty} \sum_{p,n} \frac{z_k^p}{p!}\, h_{n,o}^{(k)}\, \frac{d^p}{d(-ms)^p} \left\{ \frac{-ms - \sqrt{(ms)^2 - s_{k_\varphi}^2 - 1}}{1 - is_{k_\varphi}} \right\}^{-n}$$

The differentiation procedure in (3.10) can be simplified considerably by the approximation

$$\text{for } m \geq 2 \qquad \frac{-ms - \sqrt{(ms)^2 - s_{k_\varphi}^2 - 1}}{1 - is_{k_\varphi}} = \frac{-2ms}{1 - is_{k_\varphi}} \tag{3.11}$$

In the appendix a further simplification has been obtained for m = 1

$$\sum_n h_{n,o}^{(k)}\, \frac{d^p}{d(-s)^p} \left\{ \frac{-s - \sqrt{s^2 - s_{k_\varphi}^2 - 1}}{1 - is_{k_\varphi}} \right\}^{-n} = \sum_n \left\{ \frac{-2}{1 - is_{k_\varphi}} \right\}^p h_{n,p}^{(k)}\, \{\zeta_k(s)\}^{-n-p} \tag{3.12}$$

in which

$$\zeta_k(s) = \frac{-s - \sqrt{s^2 - s_{k_\varphi}^2 - 1}}{1 - is_{k_\varphi}} \tag{3.13}$$

$$h_{n,p}^{(k)} = \lambda_k(n + p - 3)\, h_{n-2,p-1}^{(k)} + (n + p - 1)\, h_{n,p-1}^{(k)} \tag{3.14}$$

$$\left\{ h_{n-2,p-1}^{(k)} \right\}_{\substack{n=1 \\ n=2}} = 0$$

So

$$\phi_k^o(z_k) = \sum_{n=1,2}^{\infty} h_{n,o}^{(k)}\, \sigma^{-n} + 2 \sum_{p,n} \frac{z_k^p}{p!} \left[\left\{ \frac{-2}{1-is_{k_\varphi}} \right\}^p h_{n,p}^{(k)} \left\{ \zeta_k(s) \right\}^{-n-p} + \right. \tag{3.15}$$

$$\left. h_{n,o}^{(k)} \left\{ \frac{1-is_{k_\varphi}}{2} \right\}^n (-n)(-n-1)\ldots(-n-p+1)(-s)^{-n-p} \sum_{m=2,3}^{\infty} \frac{1}{m^{n+p}} \right]$$

in which the last series is identical to the Riemann-Zeta function for n+p:

$$\sum_{m=2,3}^{\infty} \frac{1}{m^{n+p}} = \zeta(n+p) - 1 \tag{3.16}$$

(3.16) represents the influence of all the holes $m > 2$ on the stress distribution around the central hole.

In (3.15) the summation over n for $p = 0$ can be omitted since the sum is a constant, independent of z_k. This constant is not relevant for the solution of the elasticity problem.

The summations over p have to be truncated. In the present work this has been done after $p = 8$ which implies that from the expansions given in (3.3) 9 terms are taken into account.

With (3.5) and

$$H_{n,p}^{(k)} = 2 \left[h_{n,o}^{(k)} \left(\frac{1-is_{k_\varphi}}{2} \right)^{n+p} (-n)()-n-1)\ldots(-n-p+1)(-s)^{-n-p} \left\{ \zeta(n+p)-1 \right\} \right.$$

$$\left. + (-1)^p\, h_{n,p}^{(k)} \left\{ \zeta_k(s) \right\}^{-n-p} \right] \tag{3.17}$$

the complex stress functions can now be written as

$$\phi_k^o(z_k) = \sum_{n=1,2}^{\infty} h_{n,o}^{(k)} (\cos n\theta - i \sin n\theta) +$$

$$\sum_{p=1,3}^{\infty} \sum_{r=0,1}^{\frac{p-1}{2}} \frac{\lambda_k^r}{(p-r)!r!} \{(1 + \lambda_k^{p-2r}) \cos(p - 2r)\,\theta +$$

$$i\,(1 - \lambda_k^{p-2r}) \sin(p - 2r)\,\theta\} \sum_{n=1,3}^{\infty} H_{n,p}^{(k)} +$$

$$\sum_{p=2,4}^{\infty} \sum_{r=0,1}^{p/2-1} \frac{\lambda_k^r}{(p-r)!r!} \{(1 + \lambda_k^{p-2r}) \cos(p - 2r)\,\theta +$$

$$i\,(1 - \lambda_k^{p-2r}) \sin(p - 2r)\,\theta\} \sum_{n=2,4}^{\infty} H_{n,p}^{(k)} \qquad (3.18)$$

4. THE CONVERGENCE AREA OF THE COMPLEX STRESS FUNCTIONS

The elementary stress functions of the central hole converge outside and on the edge of the hole. So this edge is the inner contour of the convergence area of the stress functions of the row of holes.

The elementary functions belonging to the m-th hole

$$\phi_k^m(z_k - ms) = \sum_{n=1,2}^{\infty} g_n^{(k)}(z_k - ms)^{-n}$$

converge outside and on the edge of the m-th hole. The centre point M of the central hole is in the z_k-plane a point inside the convergence area of the elementary functions of the m-th hole, so the analytic functions may be expanded into Taylor-series in the area around M. These series converge in the z_k-plane inside a circle with a radius which is equal to the distance between M and the nearest singularity of ϕ_k^m. In the z-plane this circle represents an ellipse with axes that do not coincide with the coordinate axes in the case of complex material parameters $s_{k_\varphi} = \alpha_k + i\beta_k$.

It is obvious that the convergence areas of the holes with m = 1 are the smallest. Singularities of ϕ_k^1 only occur inside the contours of these holes. Inside a circle with centre M and a radius s-1 there are certainly no singularities. Therefore this circle will be considered as the outer contour of the convergence areas of the complex stress functions of the row of holes. In the z-plane this circle is an ellipse for which, following from $z_k = s - 1$.

- width over the X-axis is $2(s - 1)$ (4.1)

- height over the Y-axis is $\dfrac{2(s - 1)}{\sqrt{\alpha_k^2 + \beta_k^2}}$ (4.2)

It is remarked that expansions (3.3) converge rapidly for small values of z_k only. This restricts the validity of the solution of the stress problem to the edge of the central hole and its direct vicinity, especially if the pitch s is small.

5. EVALUATION OF CONSTANTS $h_n^{(k)}$ FROM THE BOUNDARY CONDITIONS

The edge of the central hole is unloaded, so in (2.1) is X = Y = 0. Hence the boundary condition formulae for the loads become

$$\begin{aligned} 2\,\mathrm{Re} \sum_{k=1,2} \phi_k(z_k) &= 0 \\ 2\,\mathrm{Re} \sum_{k=1,2} s_{k\varphi}\, \phi_k(z_k) &= 0 \end{aligned} \qquad (5.1)$$

With only normal and shear loads on the plate at infinity the complex stress functions for a row of holes are

$$\phi_k(z_k) = g_{-1}^{(k)}\, z_k + \phi_k^o(z_k) \qquad k = 1,2 \qquad (5.2)$$

in which the first term represents a homogeneous stress field and $\phi_k^o(z_k)$ is evaluated in Chapter 3.

With (2.9) for $g_{-1}^{(k)}$ substitution of (5.2) in (5.1) results in

$$\begin{aligned} 2\,\mathrm{Re} \sum_{k=1,2} \phi_k^o(z_k) &= p_{xy} \sin\theta - p_y \cos\theta \\ 2\,\mathrm{Re} \sum_{k=1,2} s_{k\varphi}\, \phi_k^o(z_k) &= p_{xy} \cos\theta - p_x \sin\theta \end{aligned} \qquad (5.3)$$

in which the summations in $\phi_k^o(z_k)$ are re-arranged as follows:

$$\phi_k^o(z_k) = \sum_{p=9,10}^{\infty} h_{p,o}^{(k)} (\cos p\theta - i \sin p\theta)$$

$$+ \sum_{p=1,3}^{7} \cos p\theta \left\{ h_{p,o}^{(k)} + (1+\lambda_k^p) \sum_{r=0,1}^{\frac{7-p}{2}} \frac{\lambda_k^r}{(p+r)!\,r!} \sum_{n=1,3}^{\infty} H_{n,p+2r}^{(k)} \right\}$$

$$+ i \sum_{p=1,3}^{7} \sin p\theta \left\{ -h_{p,o}^{(k)} + (1-\lambda_k^p) \sum_{r=0,1}^{\frac{7-p}{2}} \frac{\lambda_k^r}{(p+r)!\,r!} \sum_{n=1,3}^{\infty} H_{n,p+2r}^{(k)} \right\}$$

$$+ \sum_{p=2,4}^{8} \cos p\theta \left\{ h_{p,o}^{(k)} + (1+\lambda_k^p) \sum_{r=0,1}^{\frac{8-p}{2}} \frac{\lambda_k^r}{(p+r)!\,r!} \sum_{n=2,4}^{\infty} H_{n,p+2r}^{(k)} \right\}$$

$$+ i \sum_{p=2,4}^{\infty} \sin p\theta \left\{ -h_{p,o}^{(k)} + (1-\lambda_k^p) \sum_{r=0,1}^{\frac{8-p}{2}} \frac{\lambda_k^r}{(p+r)!\,r!} \sum_{n=2,4}^{\infty} H_{n,p+2r}^{(k)} \right\}$$

$$k = 1,2 \qquad (5.4)$$

After substitution of (5.4) into (5.3) comparison of coefficients of sines and cosines with equal coefficients of the angle θ yields:

For $p = 1, 3, 5, 7$

$$2\,\mathrm{Re} \sum_{k=1,2} \left\{ h_{p,o}^{(k)} + (1+\lambda_k^p) \sum_{r=0,1}^{\frac{7-p}{2}} \frac{\lambda_k^r}{(p+r)!\,r!} \sum_{n=1,3}^{\infty} H_{n,p+2r}^{(k)} \right\}$$

$$= \frac{p_y(p-3)(p-5)(p-7)}{48}$$

$$2\,\mathrm{Re} \sum_{k=1,2} i \left\{ -h_{p.o}^{(k)} + (1-\lambda_k^p) \sum_{r=0,1}^{\frac{7-p}{2}} \frac{\lambda_k^r}{(p+r)!\,r!} \sum_{n=1,3}^{\infty} H_{n,p+2r}^{(k)} \right\}$$

$$= \frac{-p_{xy}(p-3)(p-5)(p-7)}{48}$$

(5.5)

$$2\,\mathrm{Re}\sum_{k=1,2} s_{k\varphi}\left\{h^{(k)}_{p,o} + (1+\lambda_k^p)\sum_{r=0,1}^{\frac{7-p}{2}} \frac{\lambda_k^r}{(p+r)!\,r!}\sum_{n=1,3}^{\infty} H^{(k)}_{n,p+2r}\right\} = \frac{-p_{xy}(p-3)(p-5)(p-7)}{48}$$

$$2\,\mathrm{Re}\sum_{k=1,2} is_{k\varphi}\left\{-h^{(k)}_{p,o} + (1-\lambda_k^p)\sum_{r=0,1}^{\frac{7-p}{2}} \frac{\lambda_k^r}{(p+r)!\,r!}\sum_{n=1,3}^{\infty} H^{(k)}_{n,p+2r}\right\} = \frac{p_x(p-3)(p-5)(p-7)}{48}$$

which is a set of 16 equations with 16 unknown coefficients $h^{(k)}_{p,o}$ and $\overline{h^{(k)}_{p,o}}$. The last can be concluded from the fact that for $p \geq 9$ equations (5.3) yield zero values only of the coefficients $h^{(k)}_{p,o}$. Additionally it can be evaluated from (3.14) that the maximum value of n in $h^{(k)}_{n,p}$ and $H^{(k)}_{n,p}$ is $2p + 7$, which implies that the upper limit of n in the summations in (5.5) is $2(p + 2r) + 7$.

Since for $p = 2, 4, 6, 8$ boundary conditions (5.3) yield a set of homogeneous equations, the coefficients $h^{(k)}_{p,o}$ for these values of p must be zero. So all coefficients with even values of p are zero and the power series, representing the complex stress functions of a row of holes have odd powers only, similar to the stress functions for the single hole problem.

From (5.5) 4 coefficients $h^{(k)}_{n}$ $(k = 1,2)$ and their conjugated values can be obtained. With these coefficients solved the complex stress functions of a row of holes are known. It is obvious that in (5.5) any combination of p_x-, p_y- and p_{xy}-values may be introduced.

6. THE STRESSES

The most suitable expression of $\phi_k^o(z_k)$ for the calculation of the stresses is given in (3.15). With only odd powers of z_k and expression (3.17) for $H_{n,p}^{(k)}$ (3.15) can be simplified to

$$\phi_k^o(z_k) = \sum_{n=1,3}^{7} h_{n,o}^{(k)} \zeta_k^{-n} + \sum_{p=1,3}^{7} \frac{z_k^p}{p!} \left(\frac{2}{1-is_k}\right)^p \sum_{n=1,3}^{2p+7} H_{n,p}^{(k)} \qquad (6.1)$$

where $\phi_k^o(z_k)$ is extended from the edge of the hole to the area around the hole by replacing σ by ζ_k. Before substitution in the stress formulae (2.3) the functions must be differentiated with respect to z_k.

With $\frac{d\zeta_k}{dz_k} = \frac{\zeta_k}{\sqrt{z_k^2 - s_{k\varphi}^2 - 1}}$ (6.1) becomes after differentiation:

$$\phi_k^{o\,\prime}(z_k) = - \sum_{n=1,3}^{7} n\, h_{n,o}^{(k)} \zeta_k^{-n} (z_k^2 - s_{k\varphi}^2 - 1)^{\frac{1}{2}}$$

$$+ \sum_{p=1,3}^{7} \frac{z_k^{p-1}}{(p-1)!} \left(\frac{2}{1-is_{k\varphi}}\right)^p \sum_{n=1,3}^{2p+7} H_{n,p}^{(k)} \qquad (6.2)$$

The stresses obtained from (2.3) after substitution of (6.2) must be added to the homogeneous stresses p_x, p_y and p_{xy} in order to find the actual stresses. Since the edge of the hole is unloaded, the tangential stress can simply be found with

$$\sigma_t = \sigma_x + \sigma_y$$

7. NUMERICAL EVALUATION

For the isotropic case, which is added as a check on the adequacy of the present analysis, the next values of S/D have been chosen:

S/D = 1.11 , 1.25 , 2 , 3.33 and 5

The elasatic properties of isotropic materials result in $s_{k_\varphi} = i$, making λ_k according to (3.6) zero. For these materials it is not possible to obtain coefficients $h_{n,o}^{(k)}$ from equations (5.5). Therefore the calculations have been made with values of s_{k_φ} differing slightly from i. The coefficients $h_{n,o}^{(k)}$ for isotropic materials and different s/D values are listed in Table 2. In Table 3 the tangential stress on the edge of the central hole is compared with corresponding values from Ref. [4]. This stress is shown in the first quadrant in Fig. 1. In Fig. 12 the stress σ_y along the X-axis is given.

The calculations for the orthotropic materials have been made for the following pitch to diameter ratio's and material orientations:

S/D = 1.5 , 3 , 4.5 and ∞

$\varphi = 0°$ and $30°$

As an example the coefficients $h_{n,o}^{(k)}$ of the $(90_2^\circ/\pm 45°)_s$-laminate and one of the load conditions are listed in Table 4. In Figures 2-11 the stress σ_t on the upper half of the edge of the central hole is shown for the different laminates. The stress σ_y on the X-axis for values of x up to s/2 is shown in Figures 13-22. The stresses are made dimensionless with the stress p_y at infinity. Figures for s/D = ∞ are

not shown since they almost coincide with the figures for s/D = 4.5

From the calculated stress pattern a strength prediction has been made by applying the Tsai-Hill failure criterion. The strength values of the laminates used in the criterion, are given in Table 5. The calculated ultimate value of p_y is listed in Table 6, together with the angle θ where first significant damage occurs.

All calculations have been made with a computer program in Fortran IV which has the capability of handling complex expressions.

8. DISCUSSION OF RESULTS

- Evaluation of the solution

Except for the very small pitch s =1.11D Table 3 shows good agreement between the calculated stresses for the isotropic case and the corresponding values of Reference [4]. For s = 1.11D the approximations used in expressions (3.11) and (3.12) may not be sufficiently accurate, resulting in too high compressive stresses near $\theta = 90°$.

- Stress distributions and strength values

It should be noted that the failure criterion, used to predict the ultimate value of p_y as shown in Table 6, neglects important aspects such as three-dimensional stresses at the edge of the holes and non-linear elasticity of the laminates. Nevertheless the calculated value of $\overline{p_y}$ is a good indication for the first significant damage.

The peak stresses are always generated near the point on the edge of the hole where the direction of the highest Young's modulus is parallel to the hole boundary. Since this direction coincides with the direction of the highest strength of the laminate, the maximum tangential stress doesn't generally produce first damage. It is obvious that first damage occurs on places with unfavourable combinations of σ_t-values and laminate strength in the direction of σ_t. Mostly this is the case near points with a high shear stress in the direction of the material axes. The values of θ in Table 6 indicate that failure generally doesn't occur in the net area between the holes.

- The influence of the pitch of the holes

For the orthotropic laminates Figures 2-11 show a modest interaction between the holes for $s/D > 3$. The numerical results indicate that the

peak stresses for s/D = 3 are only about 2 percent larger than the corresponding single hole values, both for the approximately quasi-isotropic $(0°/90°/\pm45°)_s$-laminate and the laminates dominated by 90°-layers.

- The influence of the angle φ

The influence of φ on the stress distribution is rather strong in both load conditions. As was expected the effect is stronger for the laminates dominated by 90°-layers than for the laminates dominated by ±45°-layers. Although the $(0°/90°/\pm45°)_s$-laminate is approximately quasi-isotropic, its elastic constants differ slightly from the criteria for isotropy $s_k = i$. Therefore Figures 5 and 10 show some influence of φ on the stress distribution.

- The different load conditions

For $\varphi = 0$ the difference between the stress distributions in the two load conditions

- stress p_y at infinity
- stress p_y at infinity with full constraint of laterial contraction by $p_x = p_y \cdot C_{12}/C_{22}$

as well as the difference in $\bar{p}_y$ values is remarkably small, especially for the $(90_4°/\pm45°)_s$- and the $(90_2°/\pm45°)_s$-laminate. The value of θ where the predicted first damage occurs never exceeds 35°. Apparently the stresses in the area's between the holes are hardly influenced by the presence of a stress p_x at infinity. In Reference [4] it is shown that the stress concentration factor in $\theta = 90°$ for a row of holes along the X-axis in an isotropic plate loaded by p_x reduces from 3 to 1.69 if s/D decreases from infinite to the limiting value 1. In Reference [5] this decrease is called the "lee-effect" of the neighbouring holes. In the orthotropic plates with $\varphi = 0$ and bi-axial loading at

infinity the stress p_x cannot "penetrate" into the area's between the holes because of the generally low modulus of rigidity of the laminates, especially of those dominated by 90°-layers. This effect may also be called a "lee-effect" of the neighbouring holes.

For $\varphi = 30°$ the $\bar{p}_y$-values of the $(90^\circ_4/\pm 45°)_s$- and the $(90^\circ_2/\pm 45°)_s$-laminate show great differences between the two load conditions. These differences are caused by the presence of the shear stress $p_{xy} = p_y \cdot C_{26\varphi}/C_{22\varphi}$ at infinity in the plates loaded with full lateral constraint. This shear stress is able to "penetrate" between the holes since the modulus of rigidity of these laminates in X-Y-direction has improved considerably by the rotation over 30°. It is noted that, except for the $(\pm 45°)_s$-laminate, the $\bar{p}_y$-values of the laminates with lateral constraint are higher than those of the laminates without lateral constraint.

- The $(\pm 45°)_s$-laminate

Figures 17 and 22 show a property of the $(\pm 45°)_s$-laminate which is also known from the single-hole solution. For $\varphi = 0$ the maximum stress σ_y on the X-axis doesn't occur at the edge of the hole. For smaller values of s/D it may even occur in the middle of the net area between the holes.

9. CONCLUSIONS

The present approximate solution was evaluated by comparing the stresses for the isotropic case with values from literature. Except for the very small pitch of the holes s = 1.11D the agreement is good.

The influence of the pitch on the stress distribution shows a trend quite similar to that of isotropic materials, especially for $s/D \geq 3$.

The maximum tangential stress concentration at the edge of the hole is not an indication for first significant damage of the laminate. This damage occurs mostly in the vicinity of the points with the maximum shear stress in the direction of the material axes.

Rotation of the laminates dominated by 90°-layers reduces the strength considerably.

The difference between the stress distributions (and $\bar{p}_y$-values) in the two different load conditions is remarkably small in the non rotated case. In the rotated case however the laminates dominated by 90°-layers show a large difference.

10. REFERENCES

1. S.G. Lekhnitskii, Anisotropic Plates. Gordon and Breach, London 1968.

2. W.H.M. van Dreumel and J.L.M. Kamp, Non-Hookean behaviour in the fibre direction of carbon-fibre composites and the influence of fibre waviness on the tensile properties. Journal of Composite Materials, Vol. 11, October 1977.

3. O. Tamate, Einfluss einer unendlichen Reihe gleicher Kreislöcher auf die Durchbiegung einer dünnen Platte. Z. Angew. Math. u Mech., 37, 431-441, 1957.

4. P. Meyers, Doubly-periodic stress distributions in perforated plates. Thesis Delft, 1967.

5. K.J. Schulz, On the state of stress in perforated plates. Thesis Delft, 1941.

	E_α GPa	E_β GPa	$G_{\alpha\beta}$ GPa	$\mu_{\alpha\beta}$	s_1	s_2
$(90^\circ_4/\pm 45^\circ)_s$	18.75	121.31	12.81	0.0958	0.369i	1.070i
$(90^\circ_2/\pm 45^\circ)_s$	23.62	80.03	16.55	0.1955	0.112+0.728i	-0.112+0.728i
$(90^\circ/\pm 45^\circ)_s$	25.78	66.12	20.27	0.2701	0.360+0.704i	-0.360+0.704i
$(90^\circ/0^\circ/\pm 45^\circ)_s$	51.24	51.24	16.55	0.2326	0.679i	1.470i
$(\pm 45^\circ)_s$	20.43	20.43	27.74	0.7287	0.825+0.565i	-0.825+0.565i

Table 1: The laminate elastic constants and complex material parameters.

	s/D = 1.11	1.25	2	3.33	5
$h^{(1)}_{1.0}$	-24.76250	-17.33816	-12.50745	-12.54752	-12.83083
$h^{(1)}_{3.0}$	- 1.53759	- 0.11412	0.16736	0.03371	0.00757
$h^{(1)}_{5.0}$	- 0.54664	- 0.05035	0.01637	0.00120	0.00012
$h^{(1)}_{7.0}$	0.09817	0.00853	0.00151	0.00004	0.000002
$h^{(2)}_{1.0}$	23.40859	16.41795	11.92447	12.02486	12.32177
$h^{(2)}_{3.0}$	1.46109	0.09384	- 0.16611	- 0.03332	- 0.00747
$h^{(2)}_{5.0}$	0.52552	0.04662	- 0.01617	- 0.00118	- 0.00012
$h^{(2)}_{7.0}$	- 0.09895	- 0.00882	- 0.00148	- 0.00004	- 0.000002

Table 2: The coefficients $h^{(k)}_{n,o}$ of the complex stress functions $\phi^{o}_{k}(z_k)$ for 5 values of the pitch to hole diameter ratio.
Material: isotropic.

	s/D = 1.11		1.25		2		3.33	
		Ref.[4]		Ref.[4]		Ref.[4]		Ref.[4]
$\varphi = 0^o$	10.0	10.706	5.64	5.755	3.24	3.241	3.03	3.031
15^o	8.38	8.202	5.10	5.113	3.03	3.032	2.78	2.784
45^o	2.32	2.660	2.21	2.252	1.46	1.459	1.16	1.156
75^o	-0.042	-0.181	-0.179	-0.201	-0.325	-0.327	-0.517	-0.518
90^o	-0.885	-0.570	-0.583	-0.562	-0.610	-0.612	-0.779	-0.780

Table 3: The stress distribution σ_t/p_y at the hole boundaries of a row of holes for different values of S/D.

Material: Isotropic. Load: $\sigma_{y_\infty} = p_y$, $\sigma_{x_\infty} = \tau_{xy_\infty} = 0$.

	s/D = 1.5	3	4.5	∞
$h^{(1)}_{1.0}$	$3.960.10^{-2}+i.1.382.10^{0}$	$2.415.10^{-1}+i.9.187.10^{-1}$	$2.649.10^{-1}+i.8.863.10^{-1}$	$2.814.10^{-1}+i.8.706.10^{-1}$
$h^{(1)}_{3.0}$	$-4.905.10^{-2}+i.2.802.10^{-2}$	$-2.110.10^{-3}-i.9.505.10^{-4}$	$-3.935.10^{-4}-i.2.538.10^{-4}$	$-6.537.10^{-6}-i.5.017.10^{-6}$
$h^{(1)}_{5.0}$	$-9.284.10^{-3}+i.2.839.10^{-3}$	$-6.915.10^{-5}-i.7.101.10^{-5}$	$-5.157.10^{-6}-i.7.184.10^{-6}$	$-9.868.10^{-9}-i.1.694.10^{-7}$
$h^{(1)}_{7.0}$	$-1.677.10^{-3}-i.1.655.10^{-4}$	$-1.583.10^{-6}-i.3.210.10^{-6}$	$-4.230.10^{-8}-i.1.319.10^{-7}$	$-8.334.10^{-12}-i.3.827.10^{-11}$
$h^{(2)}_{1.0}$	$-7.562.10^{-1}-i.1.598.10^{0}$	$-7.752.10^{-1}-i.1.042.10^{0}$	$-7.788.10^{-1}-i.1.001.10^{0}$	$-7.831.10^{-1}-i.9.811.10^{-1}$
$h^{(2)}_{3.0}$	$4.543.10^{-2}-i.3.632.10^{-2}$	$2.252.10^{-3}+i.7.507.10^{-4}$	$4.300.10^{-4}+i.2.233.10^{-4}$	$7.062.10^{-6}+i.4.607.10^{-6}$
$h^{(2)}_{5.0}$	$9.370.10^{-3}-i.4.273.10^{-3}$	$8.165.10^{-5}+i.6.861.10^{-5}$	$6.315.10^{-6}+i.7.187.10^{-6}$	$1.246.10^{-8}+i.1.726.10^{-8}$
$h^{(2)}_{7.0}$	$1.830.10^{-3}-i.3.638.10^{-5}$	$2.094.10^{-6}+i.3.313.10^{-6}$	$6.138.10^{-8}+i.1.392.10^{-7}$	$1.353.10^{-11}+i.4.092.10^{-11}$

Table 4: The coefficients $h^{(k)}_{n,o}$ of the complex stress functions $\phi^{o}_{k}(z_k)$ for 4 pitch to hole diameter ratio's.
Material: C.F.R.P. $(90^{o}_{2}/\pm 45^{o})_{s}$-laminate, $\varphi = 30^{o}$.
Load: p_y, $p_x = p_y \cdot C_{12\varphi}/C_{22\varphi}$, $p_{xy} = p_y \cdot C_{26\varphi}/C_{22\varphi}$.

	$\bar{\sigma}_\alpha$ MPa		$\bar{\sigma}_\beta$ MPa		$\bar{\tau}_{\alpha\beta}$
	tens.	compr.	tens.	compr.	MPa
$(90^\circ_4/\pm 45^\circ)_s$	72	236	1258	818	168
$(90^\circ_2/\pm 45^\circ)_s$	212	286	1072	805	217
$(90^\circ/\pm 45^\circ)_s$	255	354	790	690	310
$(90^\circ/0^\circ/\pm 45^\circ)_s$	621	485	621	485	217
$(\pm 45^\circ)_s$	177	207	177	207	429

Table 5: Laminate strength values.

$\bar{p}_y$ in MPa	p_y, $p_x = 0$, $p_{xy} = 0$									p_y, $p_x = p_y.C12_\varphi/C22_\varphi$, $p_{xy} = p_y.C26_\varphi/C22_\varphi$								
	$\varphi = 0^o$						30^o						0^o						30^o					
	s/D=1.5		3		4.5		1.5		3		4.5		1.5		3		4.5		1.5		3		4.5	
	$\bar{p}_y$	θ^o	$\bar{p}_y$	θ^o	$\bar{p}_y$	θ^o	$\bar{p}_y$	θ^o	$\bar{p}_y$	θ^o	$\bar{p}_y$	θ^o	$\bar{p}_y$	θ^o	$\bar{p}_y$	θ^o	$\bar{p}_y$	θ^o	$\bar{p}_y$	θ^o	$\bar{p}_y$	θ^o	$\bar{p}_y$	θ^o
$(90^o_4/\pm45^o)_s$	136	25	183	25	190	25	38	25	59	25	63	25	135	25	179	25	186	25	97	175	118	0	120	0
$(90^o_2/\pm45^o)_s$	174	25	233	15	238	15	87	15	124	15	127	5	174	25	233	25	242	25	124	175	161	0	165	0
$(90^o/\pm45^o)_s$	194	15	238	0	241	0	111	15	151	15	157	15	198	25	265	0	274	0	145	0	183	5	188	5
$(90^o/0^o/\pm45^o)_s$	145	15	190	15	194	15	113	5	146	5	148	5	146	15	197	15	203	15	117	5	159	5	164	5
$(\pm45^o)_s$	60	25	82	0	83	0	56	0	73	5	74	5	61	35	94	25	99	35	50	15	69	15	72	15

Table 6: The ultimate value of p_y for two load conditions, two values of the angle φ between material axes and coordinate axes and three values of the pitch to hole diameter ratio. θ is the angle where first significant damage occurs on the edge of the central hole.

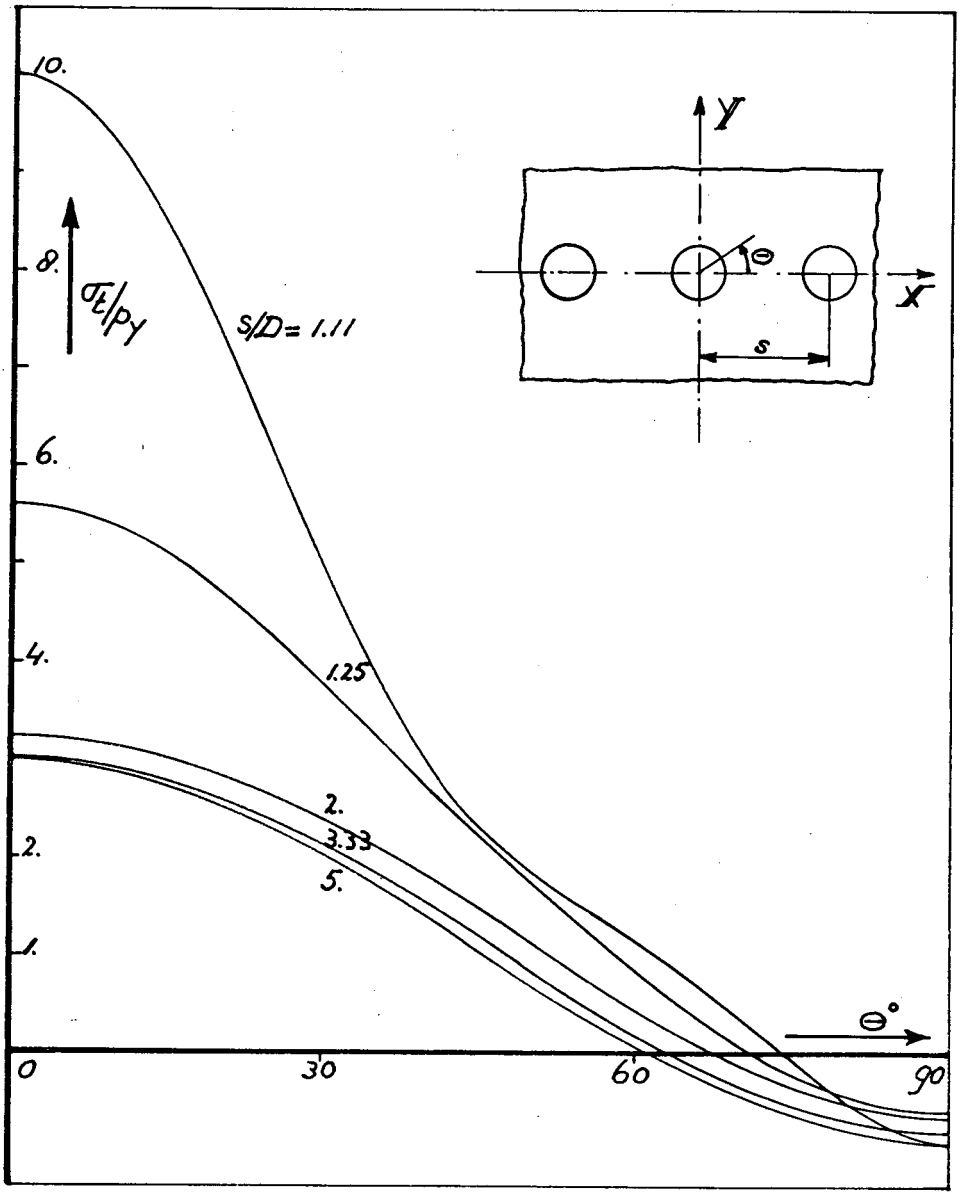

Fig. 1. The tangential stress distribution at the hole boundaries in an isotropic material. Load p_y.

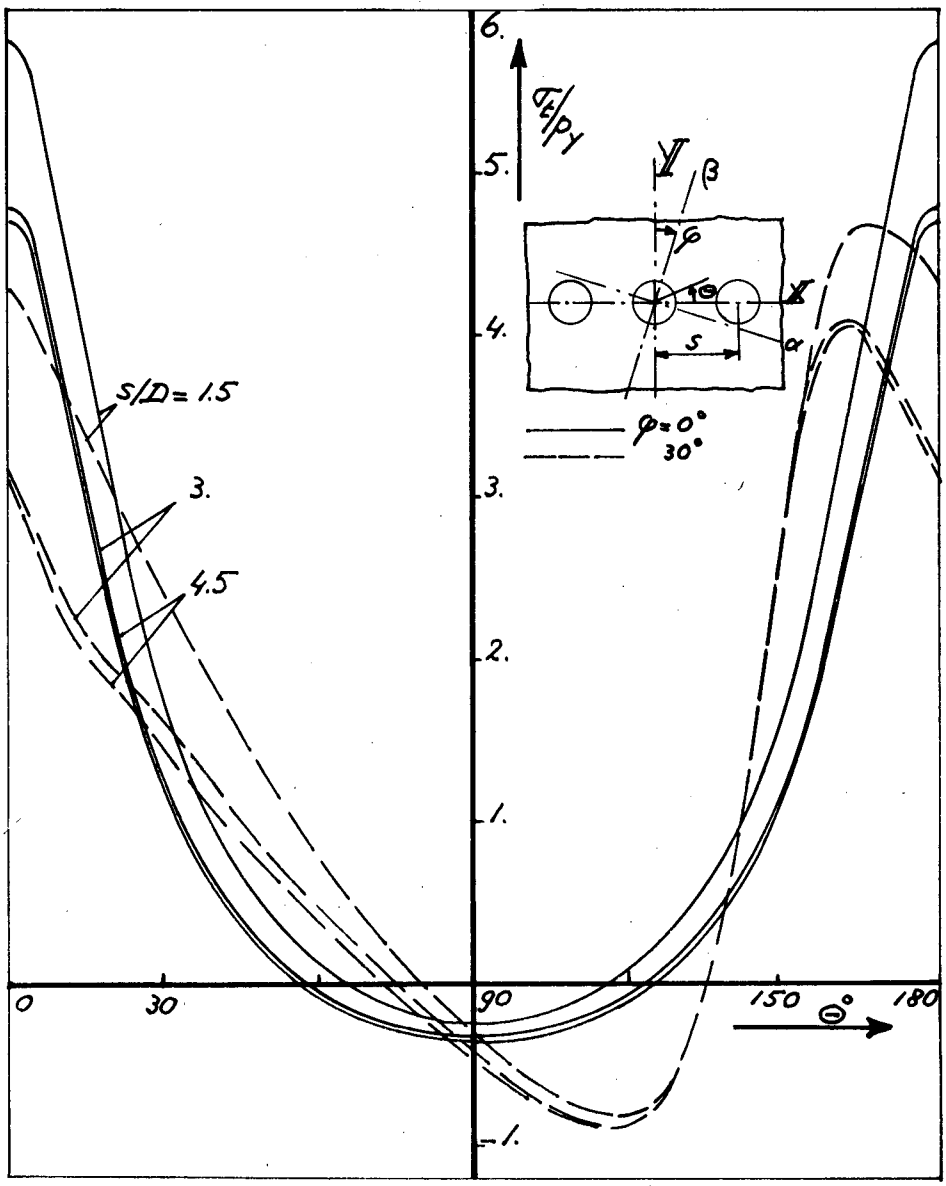

Fig. 2. The tangential stress distribution at the hole boundaries in a $(90^{\circ}_4/\pm 45^{\circ})_s$-laminate. Load p_y.

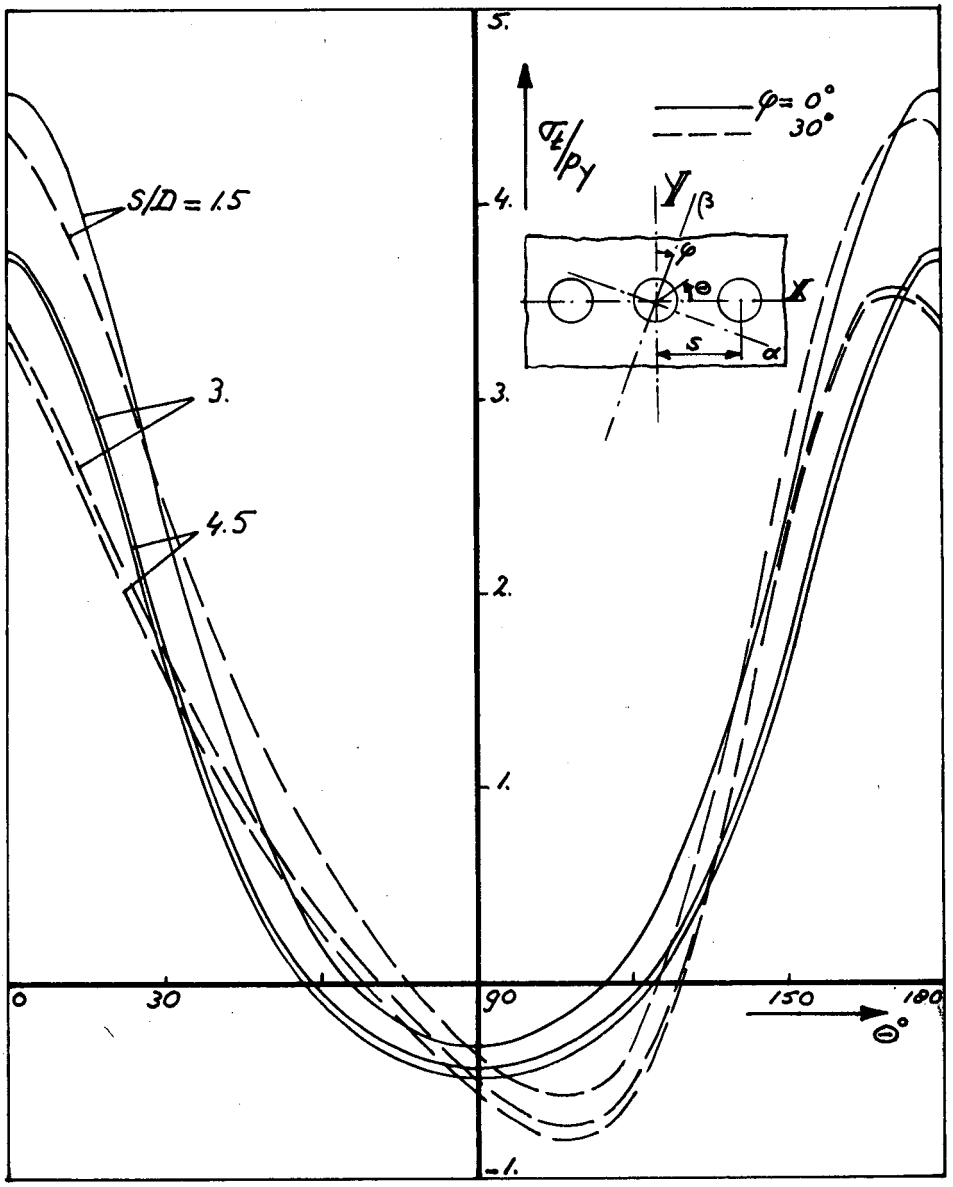

Fig. 3. The tangential stress distribution at the hole boundaries in a $(90^{\circ}_{2}/\pm 45^{\circ})_{s}$-laminate. Load p_y.

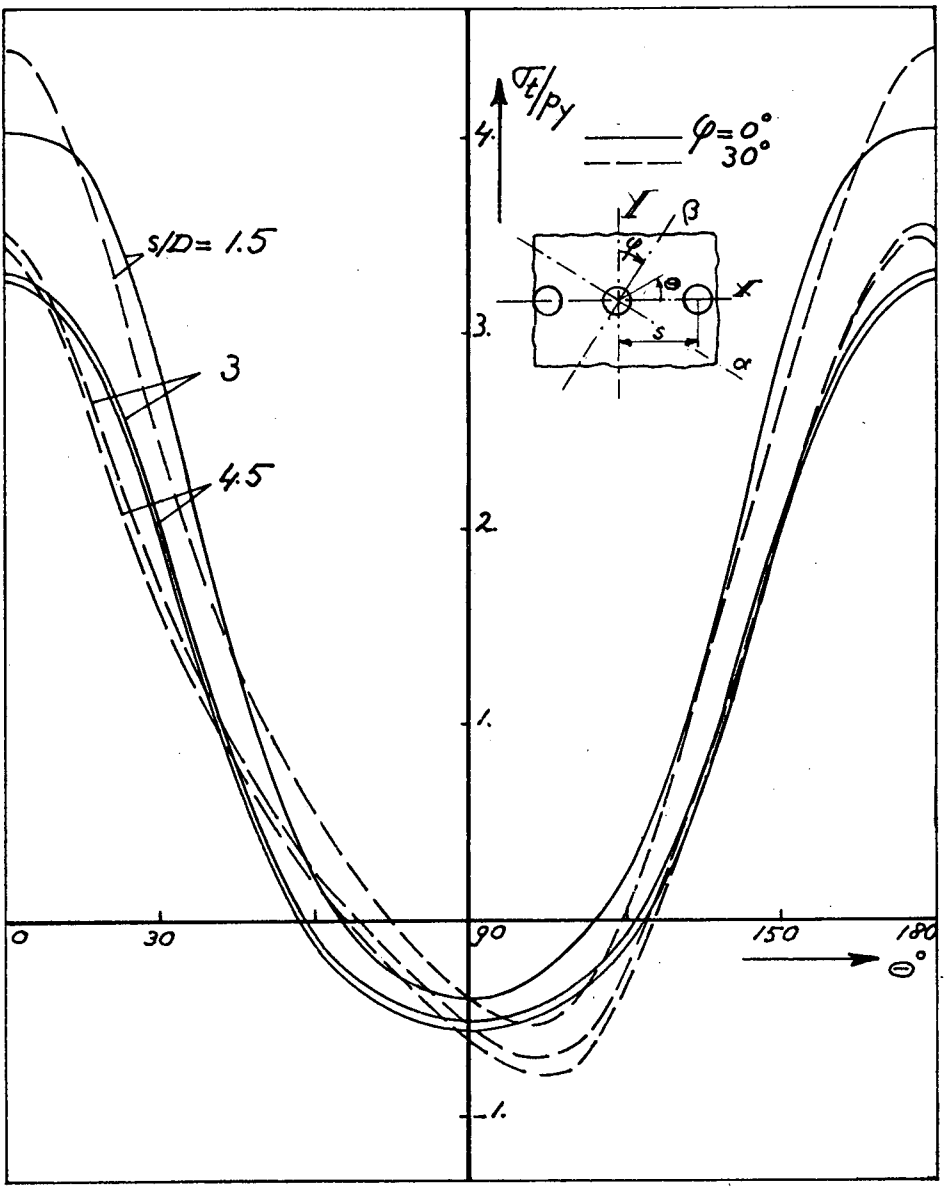

Fig. 4. The tangential stress distribution at the hole boundaries in a $(90^{o}/\pm 45^{o})_{s}$-laminate. Load p_y.

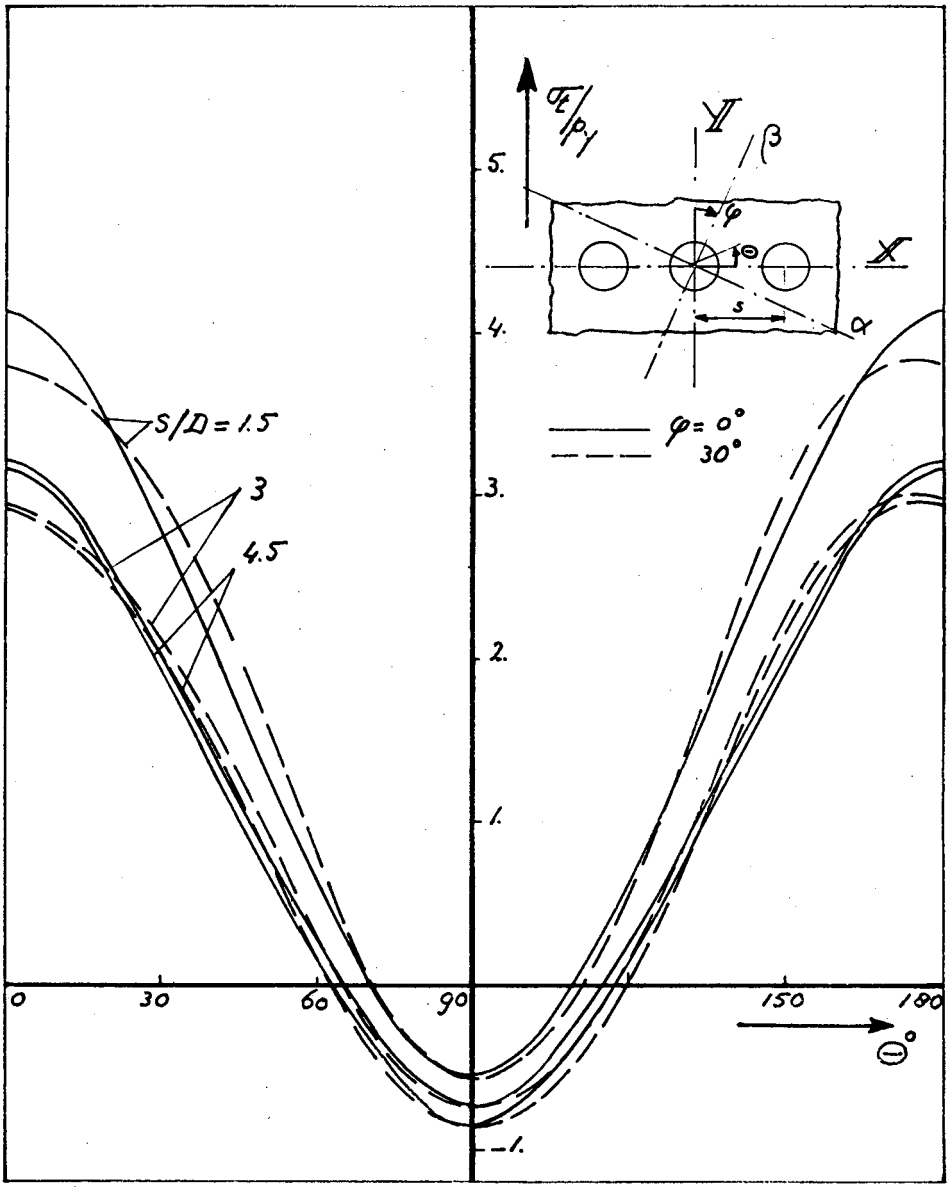

Fig. 5. The tangential stress distribution at the hole boundaries in a $(0^o/90^o/\pm 45^o)_s$-laminate. Load p_y.

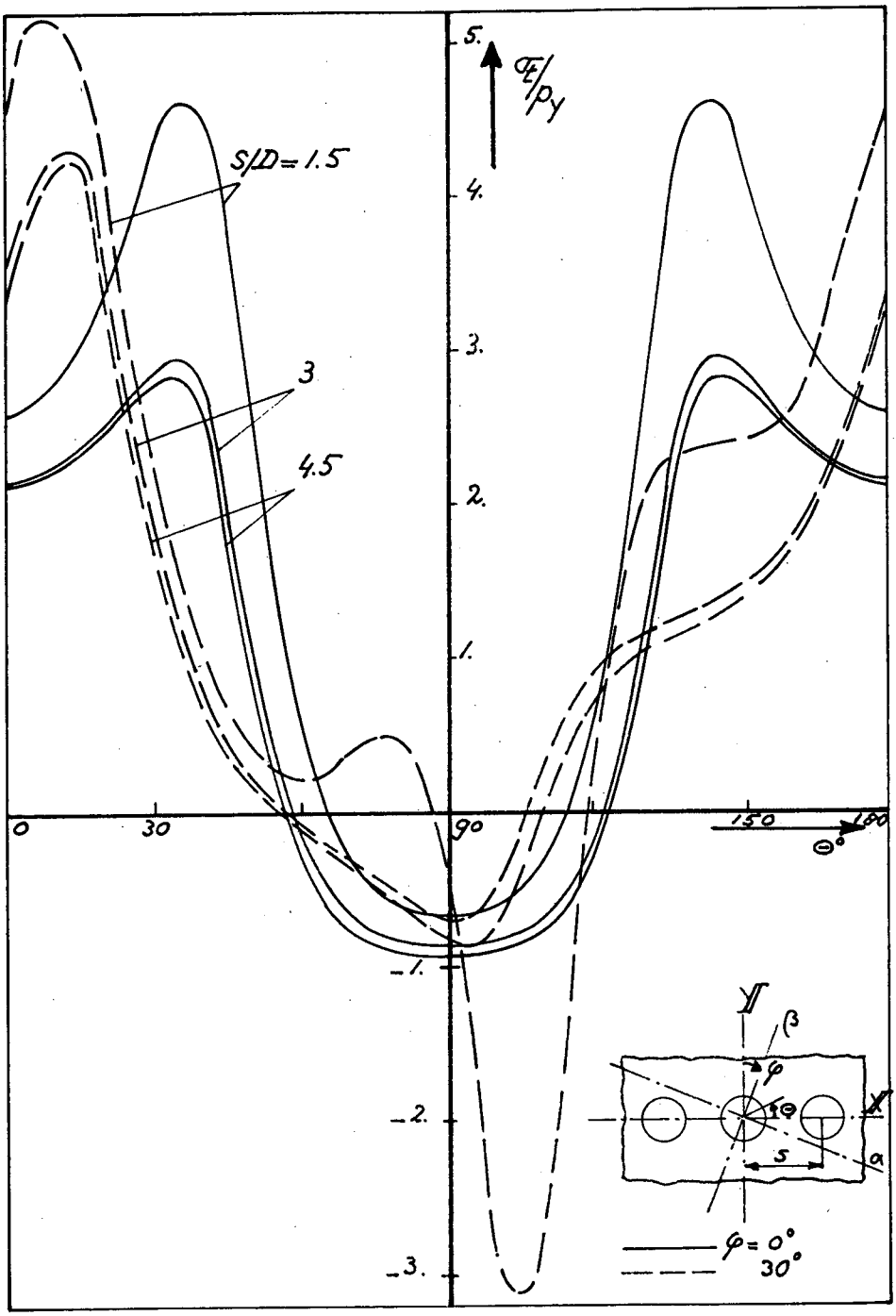

Fig. 6. The tangential stress distribution at the hole boundaries in a $(\pm 45^{o})_{s}$-laminate. Load p_y.

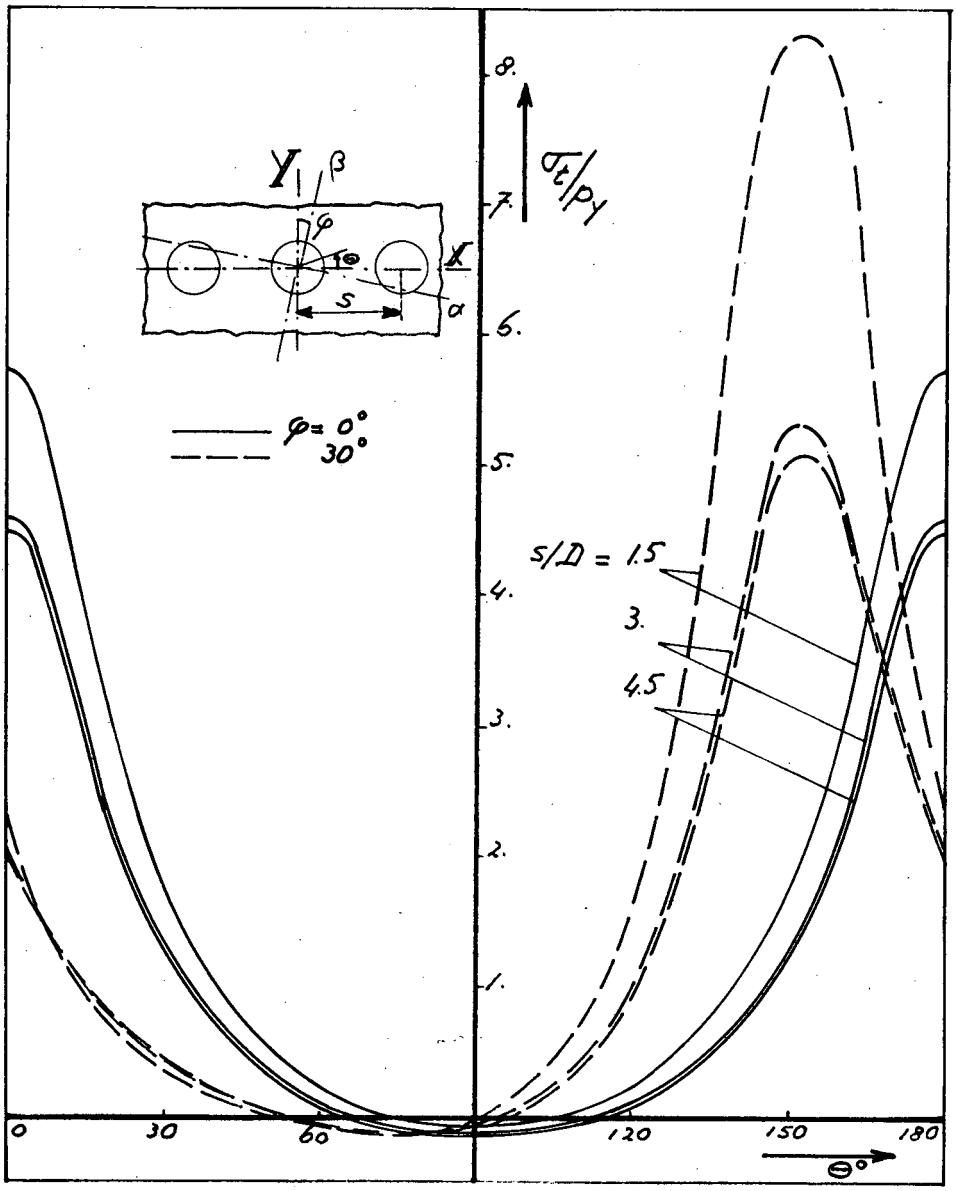

Fig. 7. The tangential stress distribution at the hole boundaries in a $(90^{\circ}_{4}/\pm 45^{\circ})_{s}$-laminate. Load p_y, $p_x = p_y \cdot C_{12}/C_{22}$, $p_{xy} = p_y \cdot C_{26}/C_{22}$.

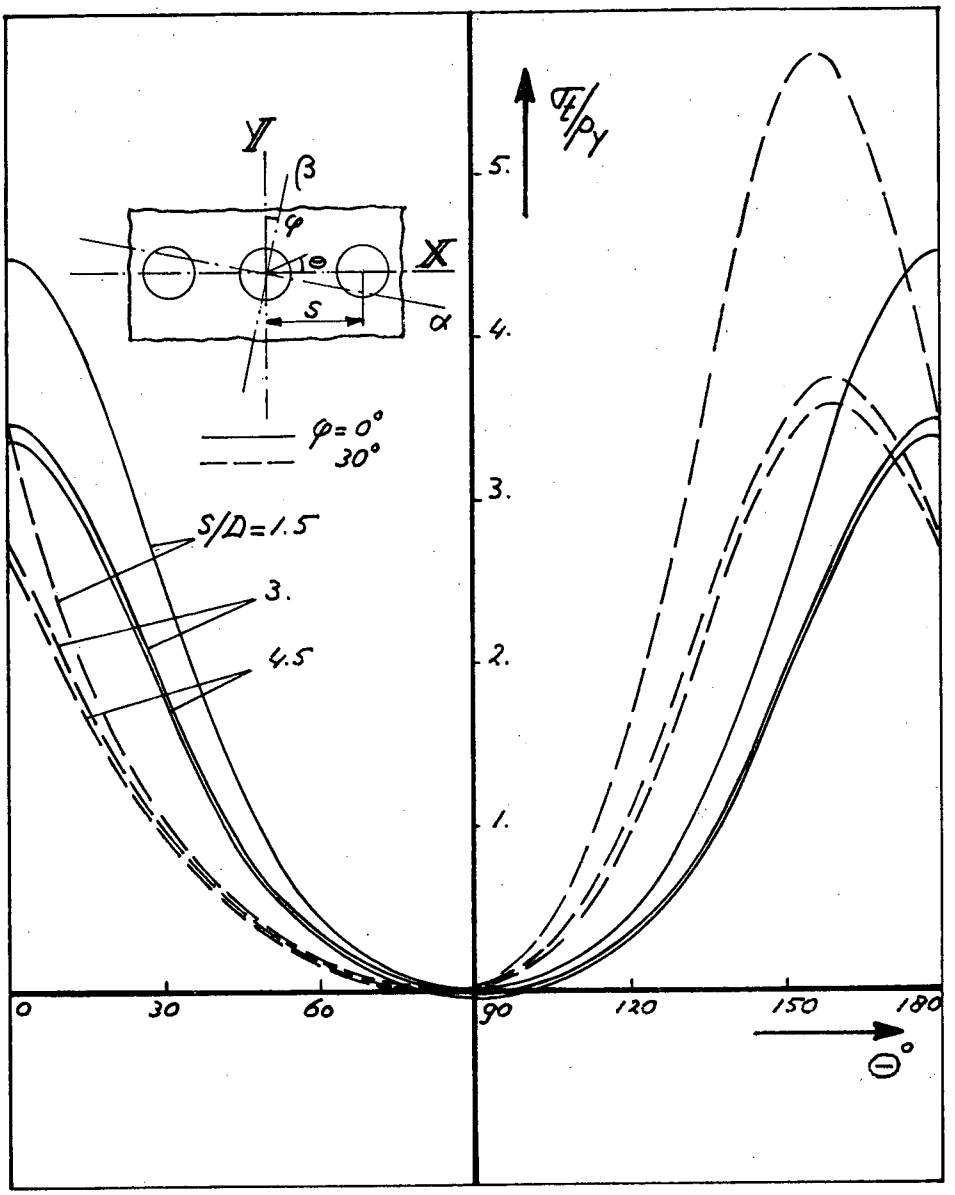

Fig. 8. The tangential stress distribution at the hole boundaries in a $(90^{\circ}_2/\pm 45^{\circ})_s$-laminate. Load p_y, $p_x = p_y \cdot C_{12}/C_{22}$, $p_{xy} = p_y \cdot C_{26}/C_{22}$.

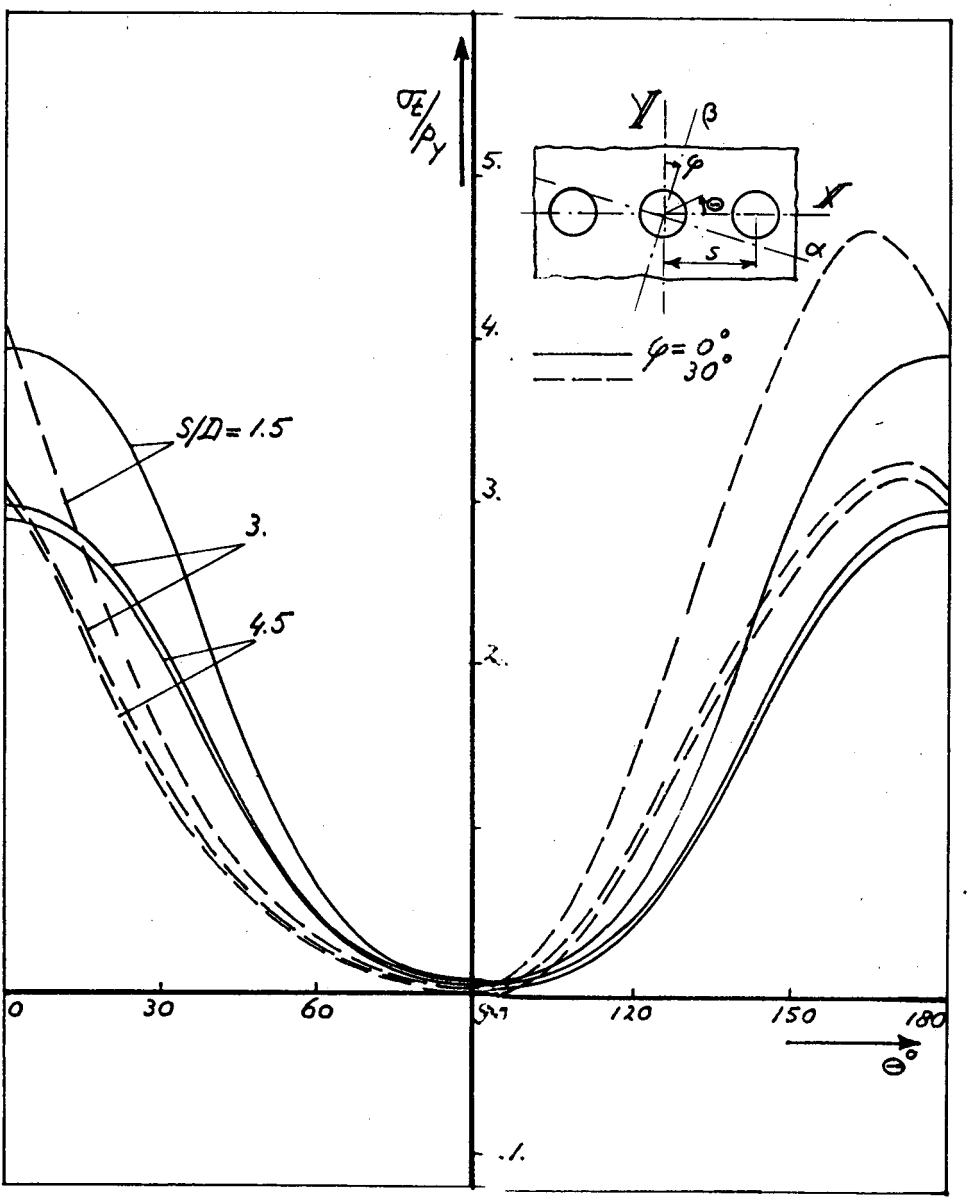

Fig. 9. The tangential stress distribution at the hole boundaries in a $(90^{o}/\pm 45^{o})_{s}$-laminate. Load p_y, $p_x = p_y \cdot C_{12}/C_{22}$, $p_{xy} = p_y \cdot C_{26}/C_{22}$.

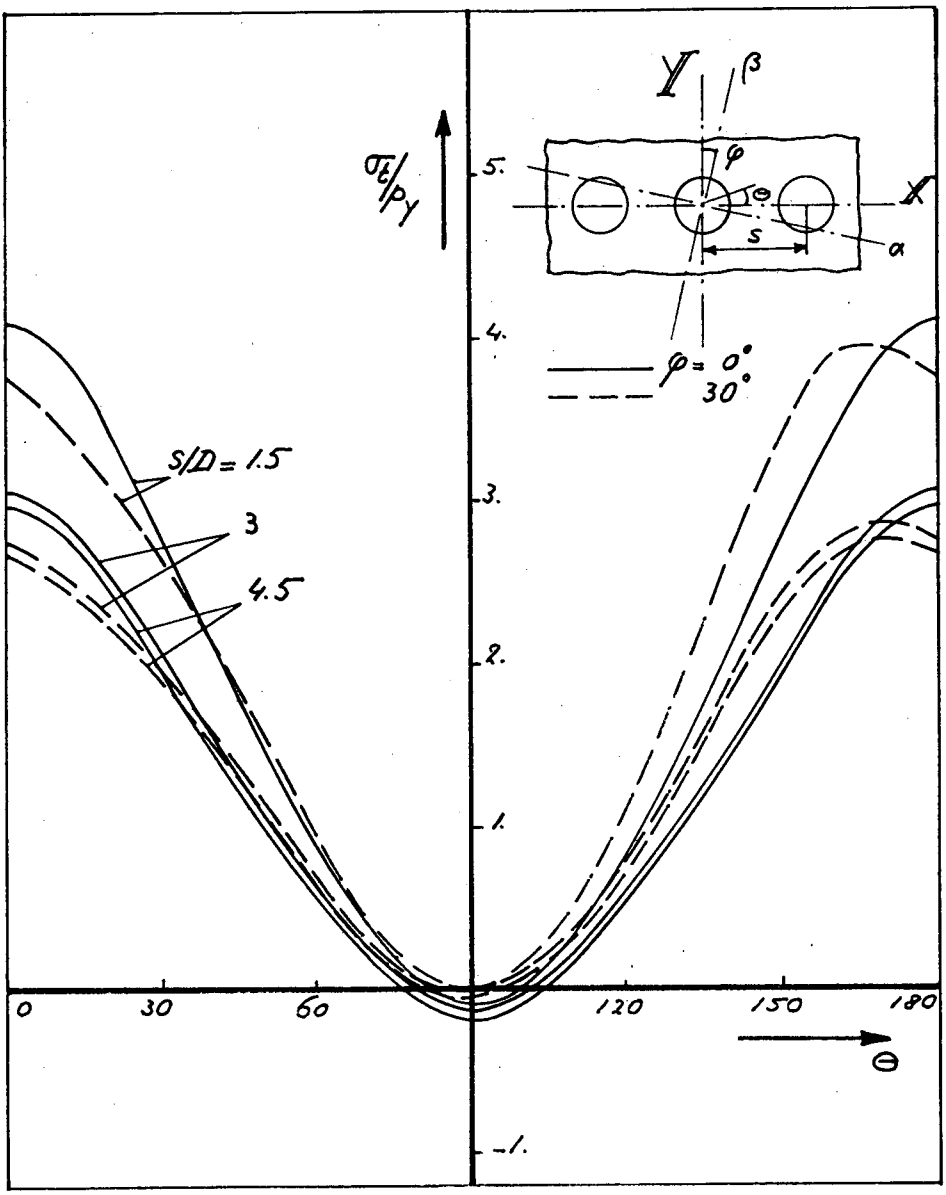

Fig. 10. The tangential stress distribution at the hole boundaries in a $(0^o/90^o/\pm 45^o)_s$-laminate. Load p_y, $p_x = p_y \cdot C_{12}/C_{22}$, $p_{xy} = p_y \cdot C_{26}/C_{22}$

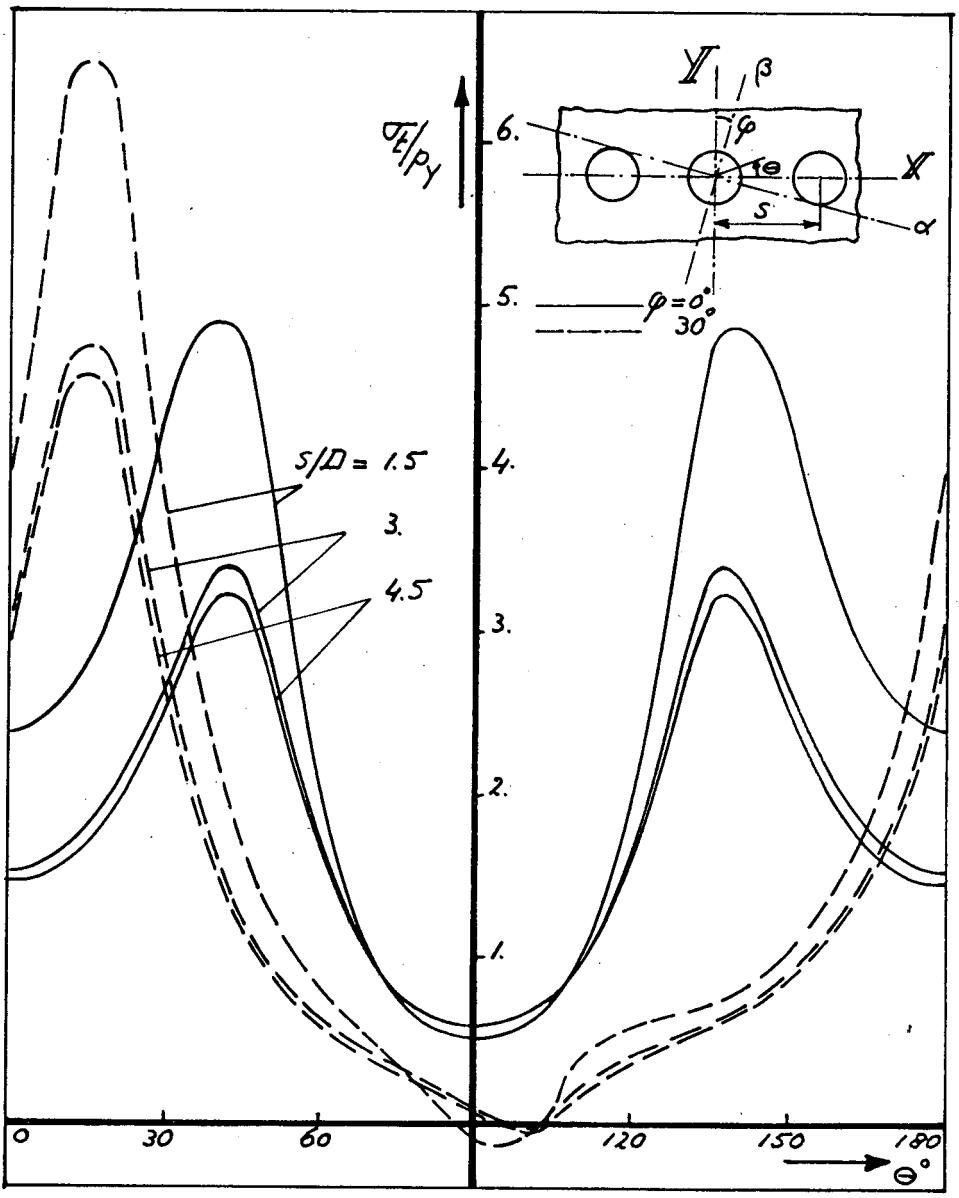

Fig. 11. The tangential stress distribution at the hole boundaries in a $(\pm 45^{o})_{s}$-laminate. Load p_y, $p_x = p_y \cdot C_{12}/C_{22}$; $p_{xy} = p_y \cdot C_{26}/C_{22}$.

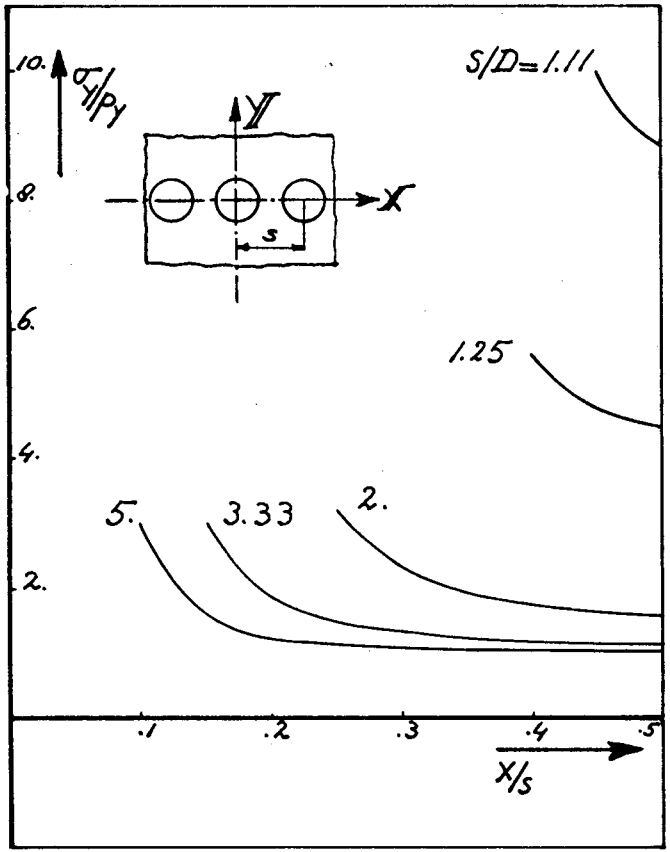

Fig. 12. The distribution of σ_y/p_y along the X-axis in an isotropic material. Load p_y.

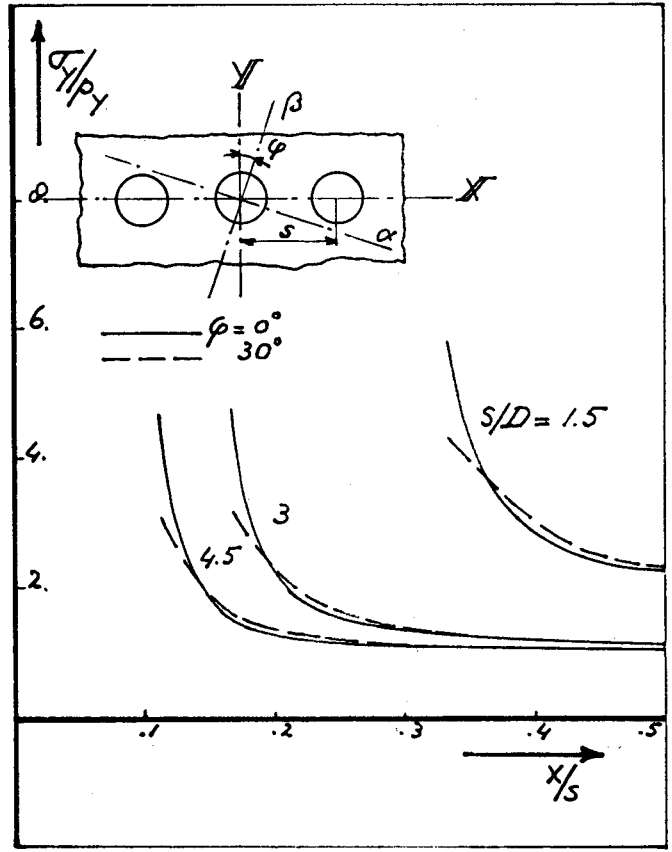

Fig. 13. The distribution of σ_y/p_y along the X-axis in a $(90^\circ_4/\pm 45^\circ)_s$-laminate. Load p_y.

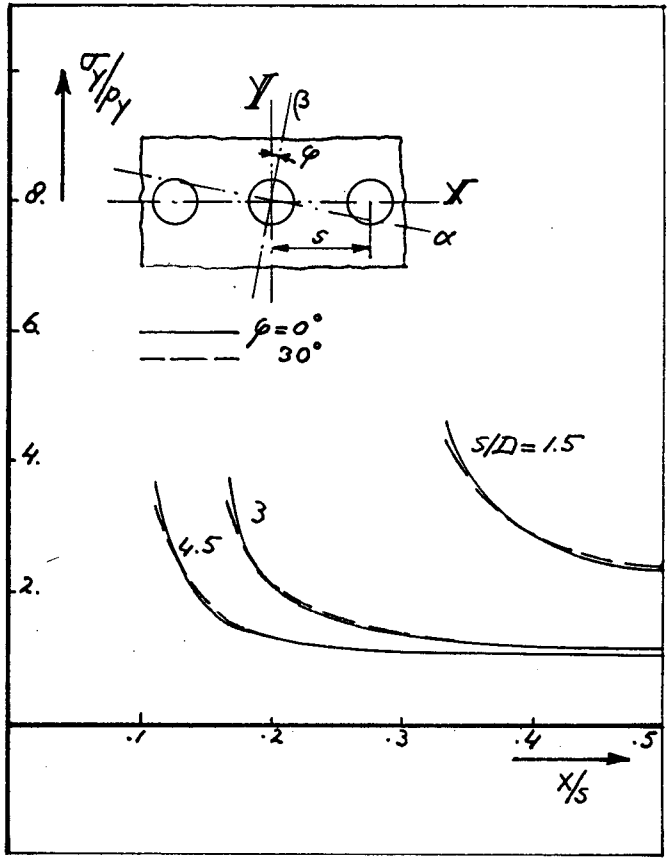

Fig. 14. The distribution of σ_y/p_y along the X-axis in a $(90^o_2/\pm 45^o)_s$-laminate. Load p_y.

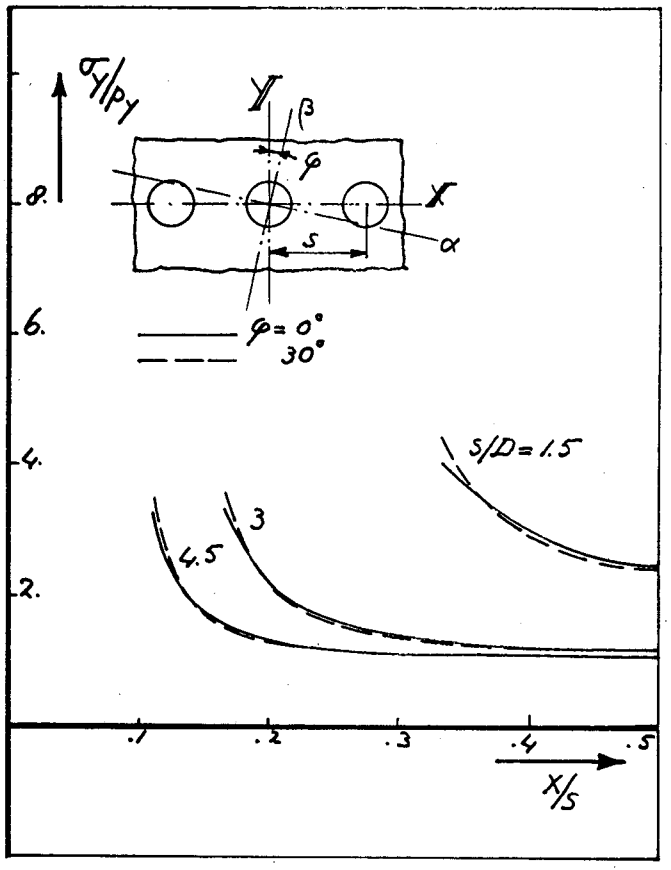

Fig. 15. The distribution of σ_y/p_y along the X-axis in a $(90^o/\pm 45^o)_s$-laminate. Load p_y.

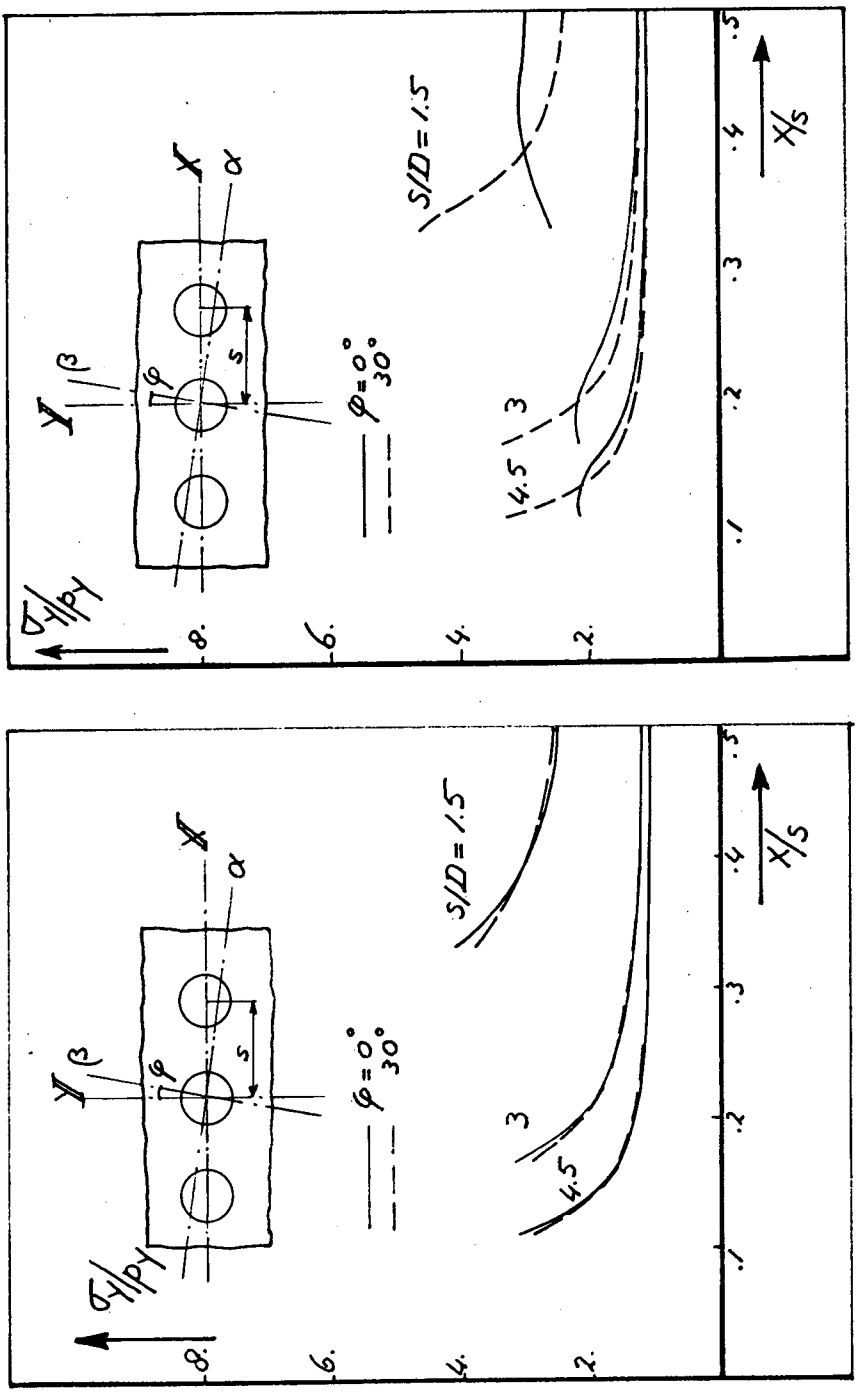

Fig. 16. The distribution of σ_y/P_y along the X-axis in a $(0^\circ/90^\circ/\pm45^\circ)_s$-laminate. Load P_y.

Fig. 17. The distribution of σ_y/P_y along the X-axis in a $(\pm45^\circ)_s$-laminate. Load P_y.

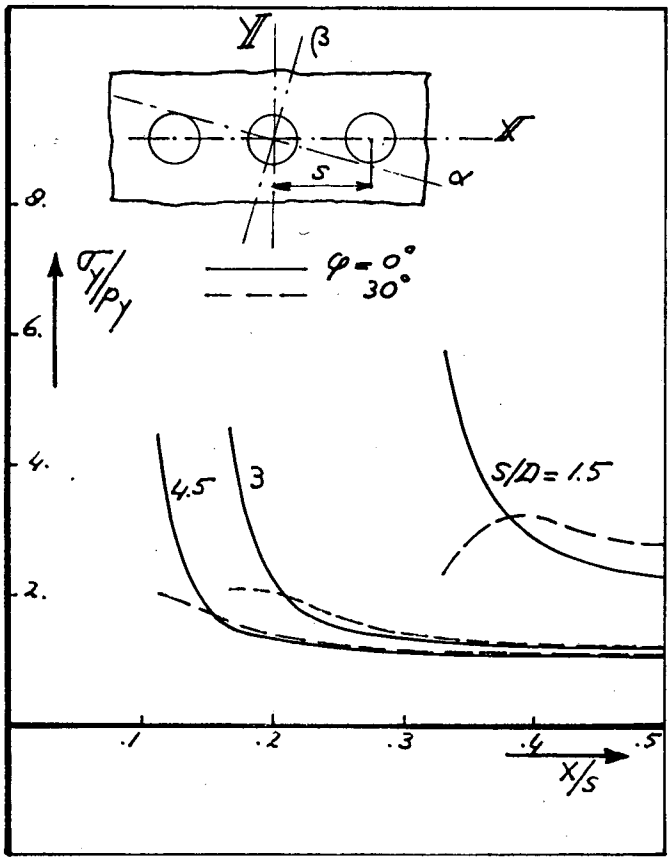

Fig. 18. The distribution of σ_y/p_y along the X-axis in a $(90^o_4/+45^o)_s$-laminate. Load p_y, $p_x = p_y \cdot \bar{C}_{12}/C_{22}$, $p_{xy} = p_y \cdot C_{26}/C_{22}$.

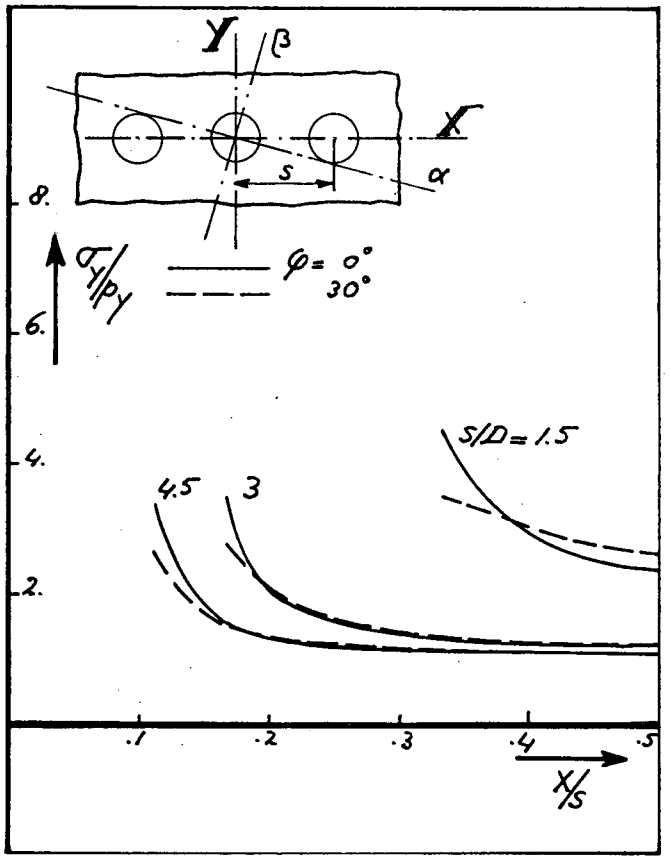

Fig. 19. The distribution of σ_y/p_y along the X-axis in a $(90^o_2/+45^o)_s$-laminate. Load p_y, $p_x = p_y \cdot \bar{C}_{12}/C_{22}$, $p_{xy} = p_y \cdot C_{26}/C_{22}$.

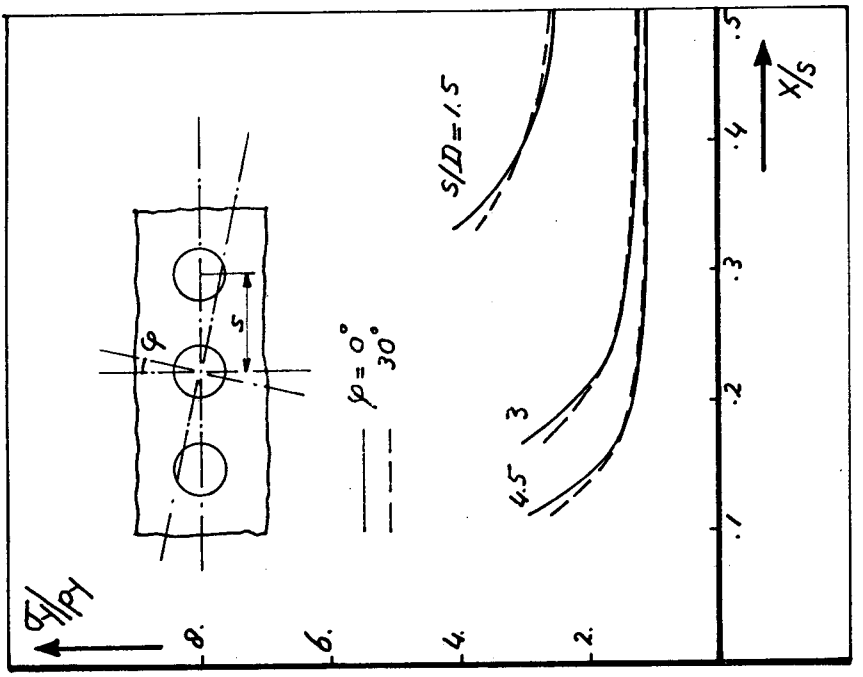

Fig. 21. The distribution of σ_y/p_y along the X-axis in a $(0^o/90^o/\pm45^o)_s$-laminate. Load P_y, $P_x = P_y \cdot \bar{C}_{12}/C_{22}$, $P_{xy} = P_y \cdot C_{26}/C_{22}$.

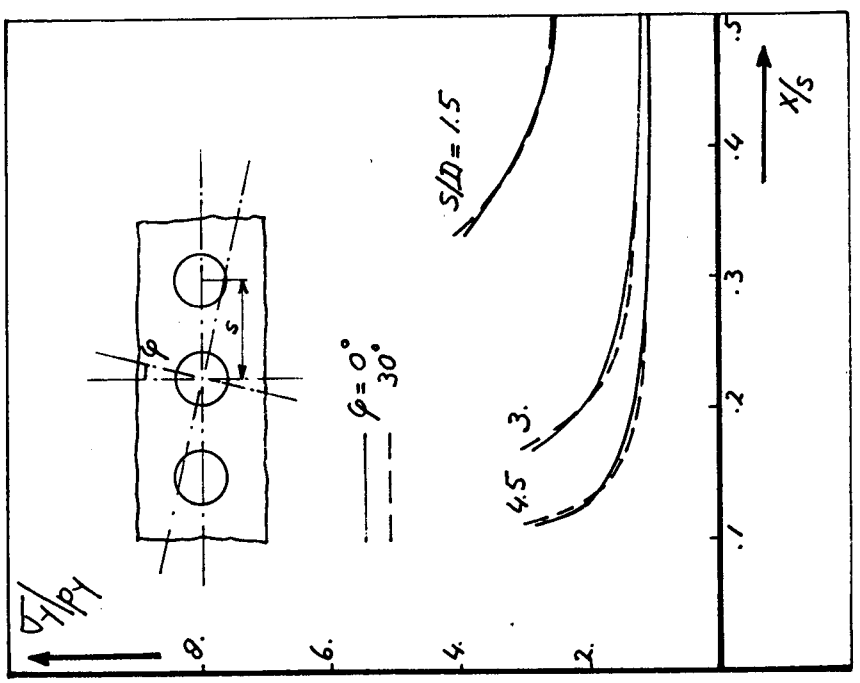

Fig. 20. The distribution of σ_y/p_y along the X-axis in a $(90^o/\pm45^o)_s$-laminate. Load P_y, $P_x = P_y \cdot \bar{C}_{12}/C_{22}$, $P_{xy} = P_y \cdot C_{26}/C_{22}$.

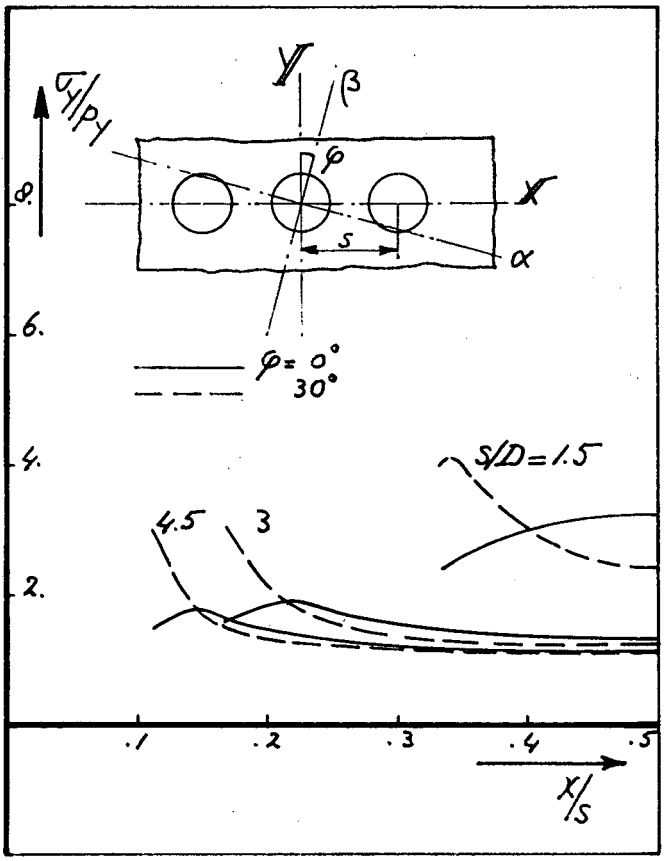

Fig. 22. The distribution of σ_y/p_y along the X-axis in a $(\pm 45^o)_s$-laminate.
Load p_y, $p_x = p_y \cdot C_{12}/C_{22}$, $p_{xy} = p_y \cdot C_{26}/C_{22}$.

APPENDIX

The expression $\sum_{n} h_{n,o}^{(k)} \frac{d^p}{d(-s)^p} \{\zeta_k(s)\}^{-n}$

According to (3.13) is

$$\zeta_k(s) = \frac{-s - \sqrt{s^2 - s_{k_\varphi}^2 - 1}}{1 - is_{k_\varphi}}$$

in which $\zeta_k(s)$ is one of the roots of the equation

$$-s = \frac{1 - is_{k_\varphi}}{2} \zeta_k(s) + \frac{1 + is_{k_\varphi}}{2} \frac{1}{\zeta_k(s)} \qquad (A.1)$$

With

$$\lambda_k = \frac{1 + is_{k_\varphi}}{1 - is_{k_\varphi}}$$

it follows from (A.1)

$$\frac{d\zeta_k(s)}{d(-s)} = \frac{2}{1 - is_{k_\varphi}} \frac{1}{1 - \lambda_k \{\zeta_k(s)\}^2} \qquad (A.2)$$

Since $\lambda_k \{\zeta_k(s)\}^{-2} < 1$ the right-hand side of expression (A.2) may be expanded into a power series

$$\frac{d\zeta_k(s)}{d(-s)} = \frac{2}{1 - is_{k_\varphi}} \left[1 + \lambda_k \{\zeta_k(s)\}^2 + \lambda_k^2 \{\zeta_k(s)\}^4 + \ldots\right]$$

which will be truncated after the second term, resulting in the approximation

$$\frac{d\zeta_k(s)}{d(-s)} = \frac{2}{1 - is_{k_\varphi}} \left[1 + \lambda_k \{\zeta_k(s)\}^2\right] \qquad (A.3)$$

The accuracy of this approximation is the smallest for low values of s and high values of s_{k_φ}. For the technically minimal pitch s = 3D and a high value $s_{k_\varphi} = 3i$ the difference between the value of (A.3) and the value of the exact expression

$$\frac{d\zeta_k(s)}{d(-s)} = \frac{-\zeta_k(s)}{\sqrt{s^2 - s_{k_\varphi}^2 - 1}}$$

is only 0.25%, so the accuracy of (A.3) will be considered as sufficient for technical purposes.

With (A.3) is now easily found

$$\sum_n h_{n,o}^{(k)} \frac{d}{d(-s)} \{\zeta_k(s)\}^{-n} = \sum_n \frac{-2n}{1-is_{k_\varphi}} h_{n,o}^{(k)} \left[\{\zeta_k(s)\}^{-n-1} + \lambda_k \{\zeta_k(s)\}^{-n-3}\right]$$

$$= \sum_n \frac{-2}{1-is_{k_\varphi}} \{\lambda_k (n-2)\, h_{n-2,0}^{(k)} + n\, h_{n,o}^{(k)}\} \{\zeta_k(s)\}^{-n-1}$$

$$= \sum_n \frac{-2}{1-is_{k_\varphi}} h_{n,1}^{(k)} \{\zeta_k(s)\}^{-n-1} \qquad (A.4)$$

in which

$$h_{n,1}^{(k)} = \lambda_k(n-2)\ h_{n-2,0}^{(k)} + n\ h_{n,o}^{(k)} \qquad (A.5)$$

and $\{h_{n-2,0}^{(k)}\}_{n=1} = 0.$

In the same way is found

$$\sum_n h_{n,o}^{(k)} \frac{d^2}{d(-s)^2} \{\zeta_k(s)\}^{-n} = \frac{d}{d(-s)} \sum_n \frac{-2}{1-is_{k_\varphi}} h_{n,1}^{(k)} \{\zeta_k(s)\}^{-n-1}$$

$$= \sum_n \left(\frac{-2}{1-is_{k_\varphi}}\right)^2 h_{n,2}^{(k)} \{\zeta_k(s)\}^{-n-2}$$

in which

$$h_{n,2}^{(k)} = \lambda_k(n-1)\ h_{n-2,1}^{(k)} + (n+1)\ h_{n,1}^{(k)}$$

and $\{h_{n-2,1}^{(k)}\}_{n=2} = 0.$

For the general term is now found

$$\sum_n h_{n,o}^{(k)} \frac{d^p}{d(-s)^p} \{\zeta_k(s)\}^{-n} = \sum_n \left(\frac{-2}{1-is_{k_\varphi}}\right)^p h_{n,p}^{(k)} \{\zeta_k(s)\}^{-n-p} \qquad (A.6)$$

where

$$h^{(k)}_{n,p} = \lambda_k(n+p-3)\, h^{(k)}_{n-2,p-1} + (n+p-1)\, h^{(k)}_{n,p-1} \tag{A.7}$$

$$\text{and } \{h^{(k)}_{n-2,p-1}\}_{\substack{n=1\\n=2}} = 0 \tag{A.8}$$

From the boundary conditions (5.4) is known that for even values of n all coefficients $h^{(k)}_{n,o}$ are zero and that the maximum odd value of n in $h^{(k)}_{n,o}$ is 7. For n in $h^{(k)}_{n,p}$ in (A.7) this results in a maximum value 21.